

**Measurement of charged fragments
production cross sections ($d\sigma/dE$) in the
interactions of C-ions with C,H,O targets**

CNAO Nov 2017 data taking

IlaMi for Roma and Milano, 2024

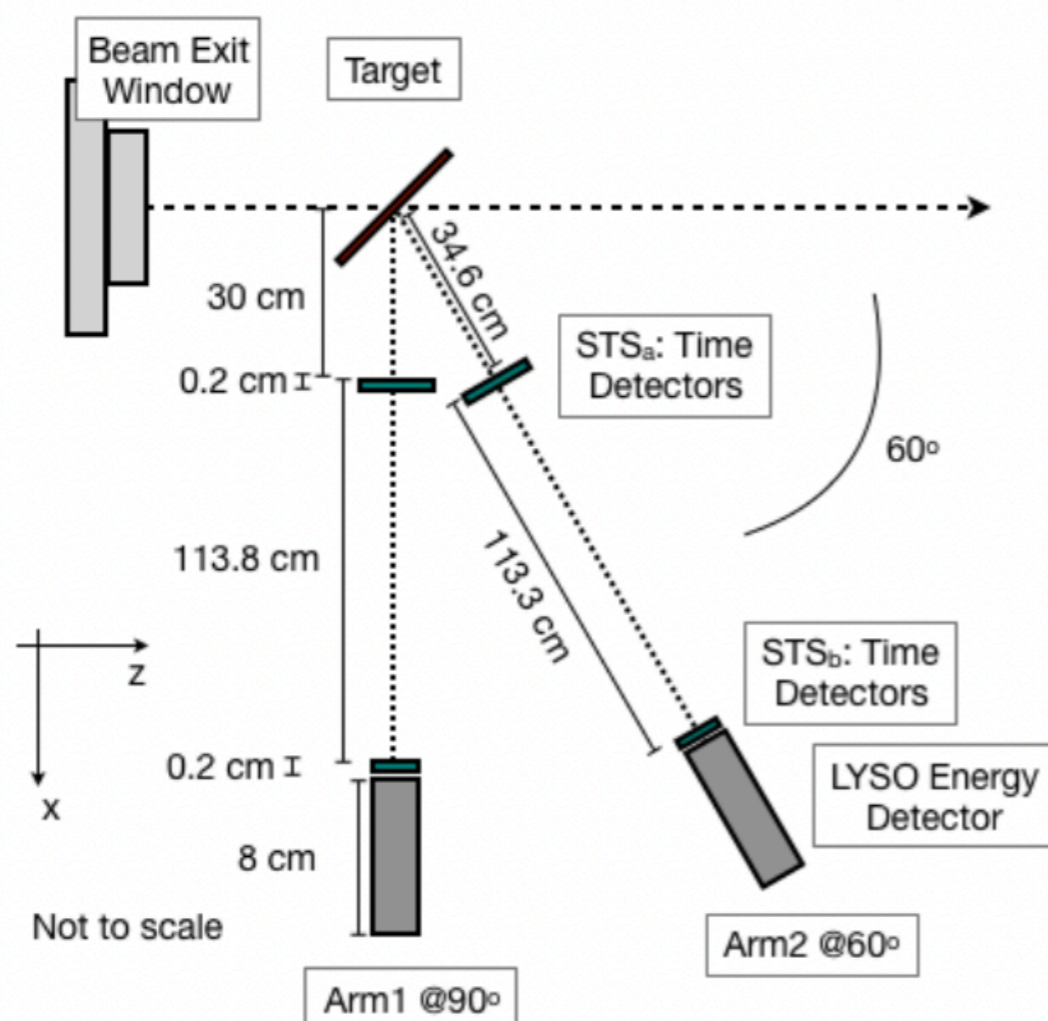


Experimental SETUP

Thin Targets based on C,H and O elements: PMMA, Graphite and Plastic Scintillator

- ❖ The fragments production ($Z=1$) has been measured as a function of the kinetic energy for 4 angles;
- ❖ The Time of Flight in thin plastic scintillators and the energy deposit in the inorganic crystals has been used for PID and kinetic energy measurements;

The thin targets (1-2 mm) do not require, as a first approximation, the implementation of a correction for the fragments absorption inside the target.



- ❖ 4 STS: thicknesses 2 mm for ToF measurements (Time Resolution $\sim 400-600$ ps) and Deposited Energy measurements (dE)
- ❖ 2 LYSO: 4x4x8 cm thick for Deposited Energy measurements (E)

**Carbon beam energies:
115,150,221,279,351 MeV/u**

**Angles:
90°/60°;
50°/32° (?)**



2020 Publication - 90°/60°

$$\frac{1}{\Delta\Omega} \frac{d\sigma}{dE_k} \left(\begin{smallmatrix} A \\ Z \end{smallmatrix} X \right) = \frac{1}{4\pi} \cdot \frac{1}{N_Y \Delta E_k} \cdot \frac{N_{AZX}(E_k)}{N_{12C}} \cdot \frac{1}{\epsilon}$$

Measurement of ^{12}C Fragmentation Cross Sections on C, O and H in the Energy Range of interest for Particle Therapy Applications.

I. Mattei¹, A. Alexandrov⁶, L. Alunni Soletizi^{21,7}, G. Ambrosi⁷, S. Argirò^{8,9}, N. Bartosik⁸, G. Battistoni¹, N. Belcarì^{10,11}, S. Biondi^{12,13}, M.G. Bisogni^{10,11}, G. Bruni¹², N. Camarlinghi^{10,11}, P. Carra^{10,11}, E. Catanzani^{21,7}, E. Ciarrocchi^{10,11}, P. Cerello⁸, A. Clozza¹⁴, S. Colombi^{15,16}, G. De Lellis^{6,17,32}, A. Del Guerra^{10,11}, M. De Simoni^{5,2}, A. Di Crescenzo^{17,6}, M. Donetti^{18,8}, Y. Dong^{1,19}, M. Durante¹⁵, A. Embriaco¹, M. Emde²⁰, R. Faccini^{5,2}, V. Ferrero^{8,9}, F. Ferroni^{2,5}, E. Fiandrini^{21,7}, C. Finck²², E. Fiorina^{18,11}, M. Fischetti^{3,2}, M. Francesconi^{10,11}, M. Franchini^{12,13}, L. Galli¹¹, V. Gentile²³, R. Hetzel²⁰, S. Hild¹⁵, E. Iarocci^{3,14}, M. Ionica⁷, K. Kanxheri⁷, A.C. Kraan¹¹, V. Lante¹⁸, A. Lauria^{17,17}, C. La Tessa^{15,16}, E. Lopez Torres^{8,24}, C. Massimi¹², M. Marafini^{4,2}, A. Mengarelli¹², R. Mirabelli^{5,2,4}, M.C. Montesi^{17,6}, M.C. Morone^{25,26}, M. Morrocchi¹¹, S. Muraro¹, L. Narici^{25,26}, A. Pastore²⁷, N. Pastrone⁸, V. Patera^{2,3,4}, F. Pennazio⁸, P. Placidi^{28,7}, M. Pullia¹⁸, L. Ramello^{8,29}, R. Ridolfi^{13,12}, V. Rosso^{10,11}, M. Rovituso¹⁵, C. Sanelli¹⁴, G. Sartorelli^{13,12}, O. Sato³⁰, S. Savazzi¹⁸, L. Scavarda^{9,8}, A. Schiavi^{3,2}, C. Schuy³¹, E. Scifoni¹⁵, A. Sciubba^{3,14,4}, A. Sécher²², M. Selvi¹², L. Servoli⁷, G. Silvestre^{21,7}, M. Sitta^{29,8}, R. Spighi¹², E. Spiriti¹⁴, G. Sportelli^{10,11}, A. Stahl²⁰, S. Tomassini¹⁴, F. Tommasino^{15,16}, G. Traini^{5,2,4}, M. Toppi^{3,14}, T. Valeri⁶, S.M. Valle¹, M. Vanstalle²², M. Villa^{12,13}, U. Weber³¹, A. Zoccoli^{12,13}, A. Sarti^{3,2,4}

Abstract—In a carbon ion treatment the nuclear fragmentation of both target and beam projectiles impacts on the dose released on the tumour and on the surrounding healthy tissues. Carbon ion fragmentation occurring inside the patient body has to be studied in order to take into account this contribution. These data are also important for the development of the range monitoring techniques with charged particles. The production of charged fragments generated by carbon ion beams of 115-353 MeV/u kinetic energy impinging on carbon, oxygen and hydrogen targets has been measured at the CNAO particle therapy center (Pavia, Italy). The use of thin targets of graphite (C), PMMA (C₂O₅H₈) and polyvinyl-toluene (plastic scintillator, C₆H₈) allowed to measure fragments production cross sections, exploiting a Time of Flight (ToF) technique. Plastic scintillator detectors have been used to perform the ToF measurements, while LYSO crystals have been used for the deposited energy measurement and to perform particle identification. Cross sections have been measured at 90 and 60 degrees with respect to the beam direction. The measured proton, deuteron and triton differential production cross sections on C, O and H, obtained exploiting the target subtraction strategy, are presented here as a function of the fragment kinetic energy.

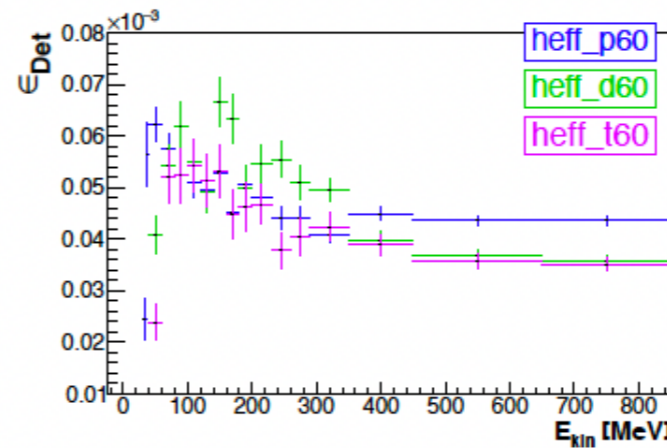
Index Terms—Scintillators Radiation Detectors for medical applications Radiation Therapy Clinical/preclinical evaluation/application studies Therapy imaging Clinical/preclinical evaluation/application studies

INTRODUCTION

PARTICLE Therapy (PT) is a well established external radiotherapy technique that exploits light charged hadron beams (as protons and carbon ions) to treat solid tumours. PT is particularly suitable in case of tumours located close to organs at risk, as well as for deep-seated or radio resistant cancers [1]. The maximum dose deposition is concentrated in

- Zid from STS detectors
- Aid from LYSO detector

Detection Efficiency from p,d,t FLAT MC



E_{kin}@Gen from analytical correction of E_{kin}@Meas

- Selection (mixing) Efficiency from FULL MC

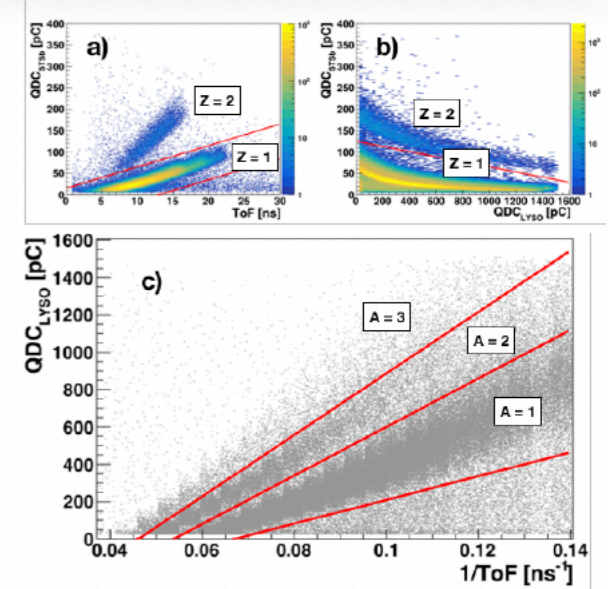


Figure 3. a) Top Left. The energy loss in the STS_b (in pC) is shown as a function of the ToF for the measured particles. b) Top Right. The energy loss in the STS_b (in pC) is shown as a function of E (in pC). c) Bottom. The Z = 1 fragments selected from a) and b) are separated in mass (A = 1, A = 2 and A = 3) using the bands identified by the red lines. Data refer to the 60 degrees sample.

$$\epsilon_{mix} = \begin{pmatrix} \epsilon^{pp} & \epsilon^{pd} & \epsilon^{pt} \\ \epsilon^{dp} & \epsilon^{dd} & \epsilon^{dt} \\ \epsilon^{tp} & \epsilon^{td} & \epsilon^{tt} \end{pmatrix}$$

Table III
PARTICLE IDENTIFICATION EFFICIENCY: SELECTION EFFICIENCIES EVALUATED FOR BOTH 90° AND 60° DETECTION CONFIGURATIONS.

E_{kin}^C [MeV/u]	ϵ^{pp} [%]	ϵ^{dd} [%]	ϵ^{tt} [%]
90°			
115	95 ± 5	89 ± 9	85 ± 12
153	95 ± 5	85 ± 14	91 ± 6
221	94 ± 5	85 ± 12	86 ± 10
281	94 ± 5	84 ± 12	71 ± 31
353	94 ± 5	84 ± 14	81 ± 15
60°			
115	95 ± 4	78 ± 21	76 ± 32
153	95 ± 5	77 ± 22	83 ± 17
221	95 ± 5	75 ± 23	73 ± 32
281	95 ± 5	75 ± 24	76 ± 26
353	94 ± 5	75 ± 24	69 ± 37

* corresponding author, please mail to: michela.marafini@roma1.infn.it

¹ INFN, Section of Milano - Milano, Italy
² INFN, Section of Roma1 - Roma, Italy
³ Dipartimento di Scienze di Base e Applicate per l'Ingegneria (SBAAI) - Roma, Italy
⁴ Museo Storico della Fisica e Centro Studi e Ricerche Enrico Fermi, Roma, Italy
⁵ Dipartimento di Fisica, Università di Roma "La Sapienza" - Roma, Italy
⁶ INFN, Section of Napoli - Napoli, Italy
⁷ INFN, Section of Perugia - Perugia, Italy
⁸ INFN, Section of Torino - Torino, Italy
⁹ Dipartimento di Fisica, Università di Torino - Torino, Italy
¹⁰ Dipartimento di Fisica, Università di Pisa - Pisa, Italy
¹¹ INFN, Section of Pisa - Pisa, Italy
¹² INFN, Section of Bologna - Bologna, Italy
¹³ Dipartimento di Fisica, Università di Bologna - Bologna, Italy
¹⁴ INFN, Laboratori Nazionali di Frascati, Frascati, Italy
¹⁵ INFN-TIFPA, Trento Institute for Fundamental Physics and Applications, Trento, Italy
¹⁶ Dipartimento di Fisica, Università di Trento - Trento, Italy
¹⁷ Dipartimento di Fisica, Università di Napoli - Napoli, Italy
¹⁸ Centro Nazionale di Adroterapia Oncologica (CNAO), Pavia, Italy
¹⁹ Dipartimento di Fisica, Università di Milano - Milano, Italy
²⁰ RWTH Aachen University, Physics Institute III B, Aachen, Germany
²¹ Dipartimento di Fisica e Geologia, Università di Perugia - Perugia, Italy
²² Université de Strasbourg, CNRS, IPHC UMR 7871, F-67000 Strasbourg, France
²³ Gran Sasso Science Institute, L'Aquila, Italy
²⁴ CEADEN, Havana, Cuba
²⁵ Dipartimento di Fisica, Università di Roma "Tor Vergata" - Roma, Italy
²⁶ INFN, Section of Roma Tor Vergata - Roma, Italy
²⁷ INFN, Section of Bari - Bari, Italy
²⁸ Dipartimento di Ingegneria, Università di Perugia - Perugia, Italy
²⁹ Dipartimento di Scienze e Innovazione Tecnologica, Università Piemonte Orientale-Alessandria, Italy
³⁰ Department of Physics, Nagoya University - Nagoya, Japan
³¹ Gesellschaft für Schwerionenforschung (GSI) - Darmstadt, Germany
³² CERN, Geneva, Switzerland

Cross section 2024

~ same as before

- DATA @ 90°/60°/50°/32°
- DATA-MC comparison
- Zid from STS detectors
- Aid from LYSO detector
- **Detection efficiency from FULL MC**
- **Selection Efficiency (mixing) binned in Ekin**
- **UNFOLDING to compute Ekin gen from Ekin meas**

$$\frac{d\sigma}{dE_k} \left(\frac{A}{Z} X \right) = \frac{1}{\Delta\Omega} \cdot \frac{\text{Purity}}{N_Y \Delta E_k} \cdot \frac{N_{\frac{A}{Z}X}(E_k)}{N_{12C}} \cdot \frac{1}{\epsilon}$$

$$\epsilon = \epsilon_{Det} \cdot \epsilon_{Sel} \cdot \epsilon_{DT}$$

Full simulation (C on Targets ~1.e¹⁰ primaries) to calculate the trigger+detection efficiency

Measurements of the DAQ dead time for each run (rate dependent)

Full simulation (C on Targets ~1.e¹⁰ primaries). On the E (and dE) vs ToF distributions, application of the PID selections tuned from data: evaluation of fragments (p, d, t) mis-identification.

Cross section 2024

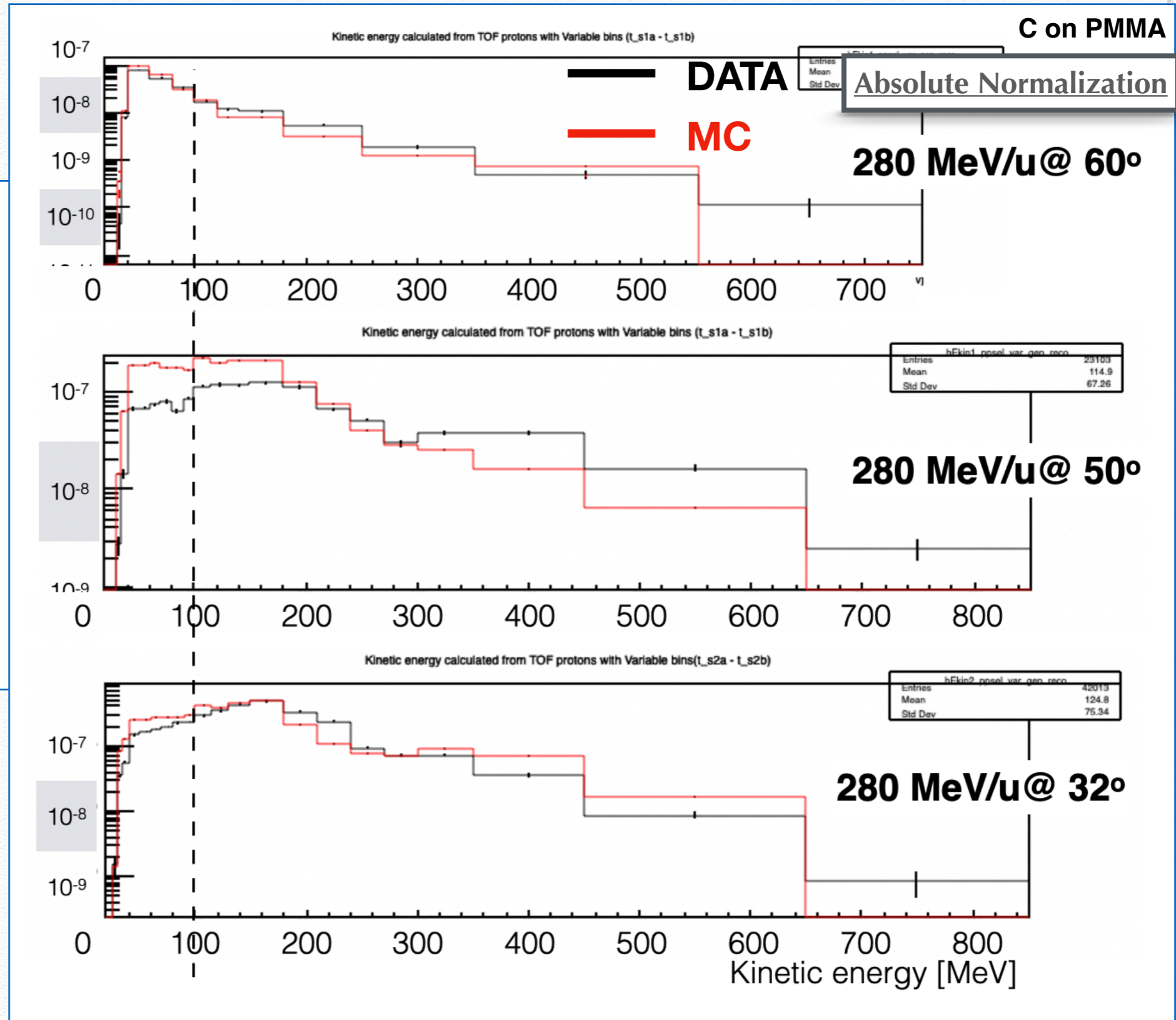
DATA @ 90°/60°/50°/32° and DATA-MC comparison

BUT

DATA @ 50°

show some issues:
HW problems (not identified) OR not the right angle (range spanned 30°-38° & 45°-54°)
OR both

not publishable

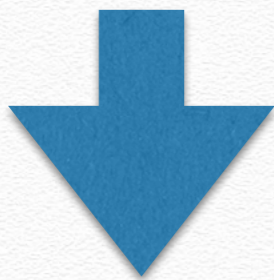


Cross section 2024

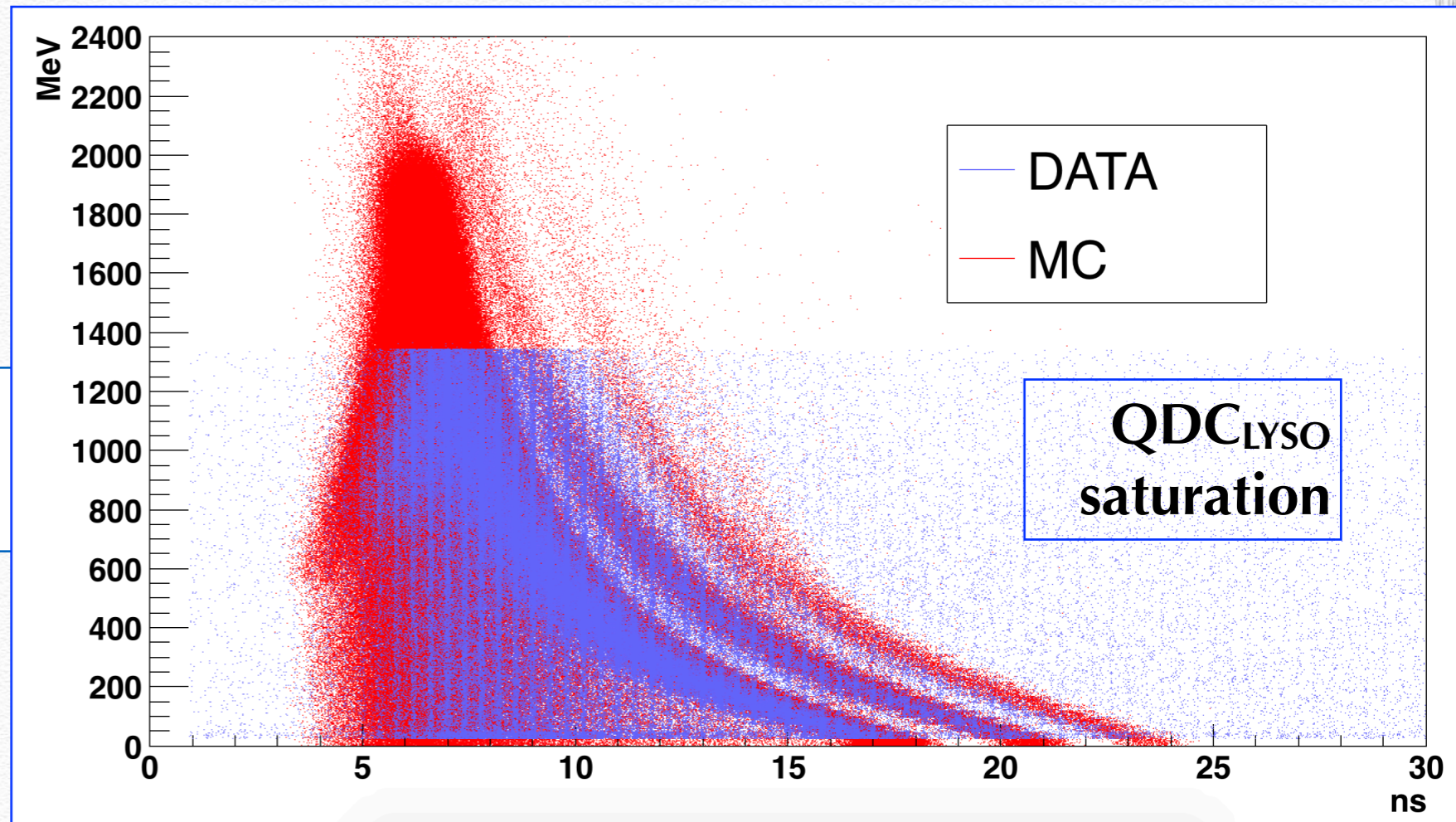
DATA @ 90°/60°/50°/32° and DATA-MC comparison

BUT

DATA @ 32°
have a QDC saturation



publication before the related ToF



Cross section 2024 - The FORMULA

The ^{12}C fragmentation cross sections for a ${}^A_Z X$ fragment are obtained as:

$$\frac{d\sigma}{dE_k} \left(\begin{smallmatrix} A \\ Z \end{smallmatrix} X \right) = \frac{N_{\begin{smallmatrix} A \\ Z \end{smallmatrix} X}(E_k)}{\Delta E_k} \cdot \frac{\text{Purity}}{N_{12\text{C}} N_Y} \cdot \frac{1}{\epsilon}$$

**Particle identification (Z,A):
same as old analysis.**

**Unfolding to compute $E_{kin\ gen}$
from $E_{kin\ meas}$.**

**Purity correction instead of
correcting for the off-diagonal
elements of the mixing matrix
(same concept, different
application)**

**For fw Angles:
NO DATA for
C 221 MeV/u
CH 150,221 MeV/u**



Cross section 2024 - YIELD

From a study on DATA available statistics (raw yield), it is possible to perform the DATA analysis of:

- **90-60: All Targets, all Beam Energies**
- **32: C no 221, CH no 150-221**

- **p: 90 - 60 - 32**
- **d: 90 integral - 60 - 32**
- **t: 60 - 32**

Cross section 2024 - Unfolding the Raw YIELD

To obtain the E_{kin} @ generation of detected particles, we need to UNFOLD the measured E_{kin} (from TOF).

The UNFOLDING ingredients are:

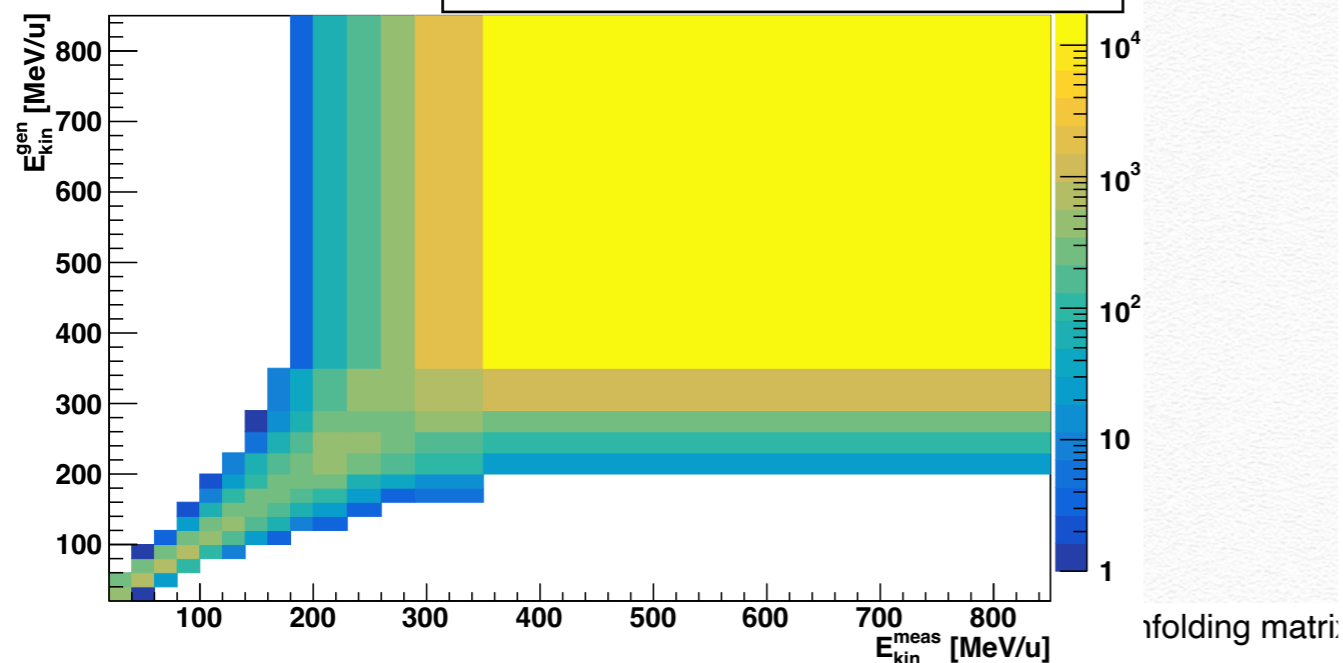
- **unfolding matrix: probability matrix that, given a measured E_{kin} , tells you the generation E_{kin}**
- **Measured E_{kin} distribution: the distribution to be unfolded**
- **Generation E_{kin} distribution: the distribution to compare with the unfolded one**

UNFOLDING

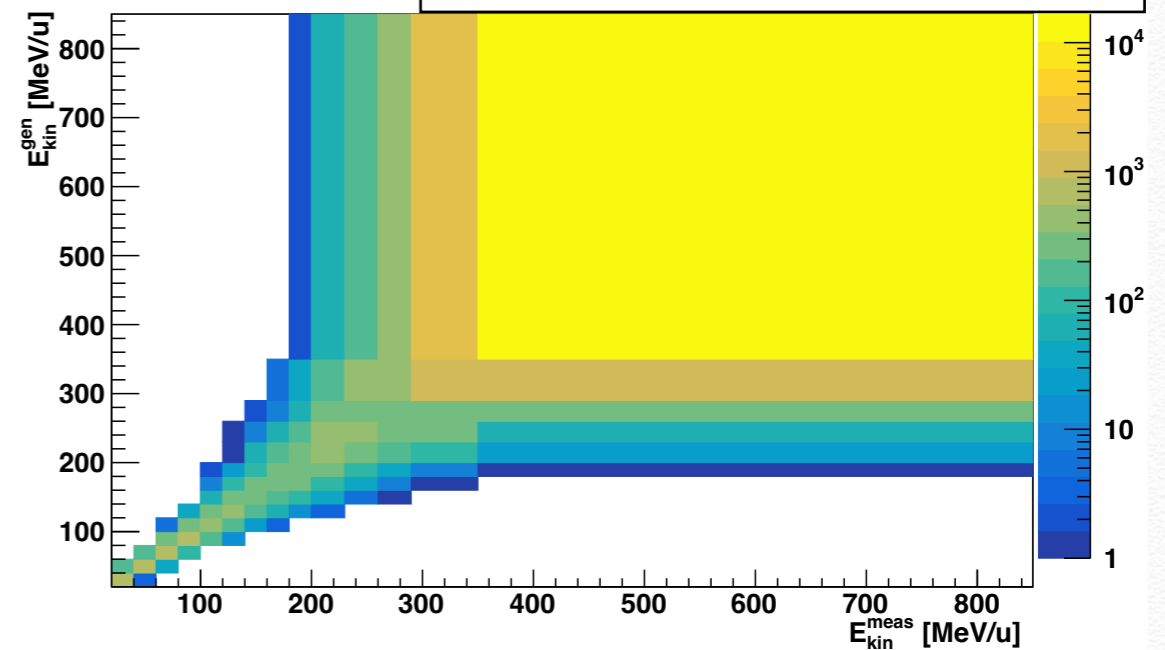
- Same x-y ranges and variable binning of FULL MC/DATA spectra

Unfolding Matrix (E_{kin}^{gen} vs E_{kin}^{meas}) from **FLAT** simulations: p, d, t generated within the PMMA + C + CH targets, with FLAT E_{kin} spectrum (5 MeV/u - 1GeV/u)

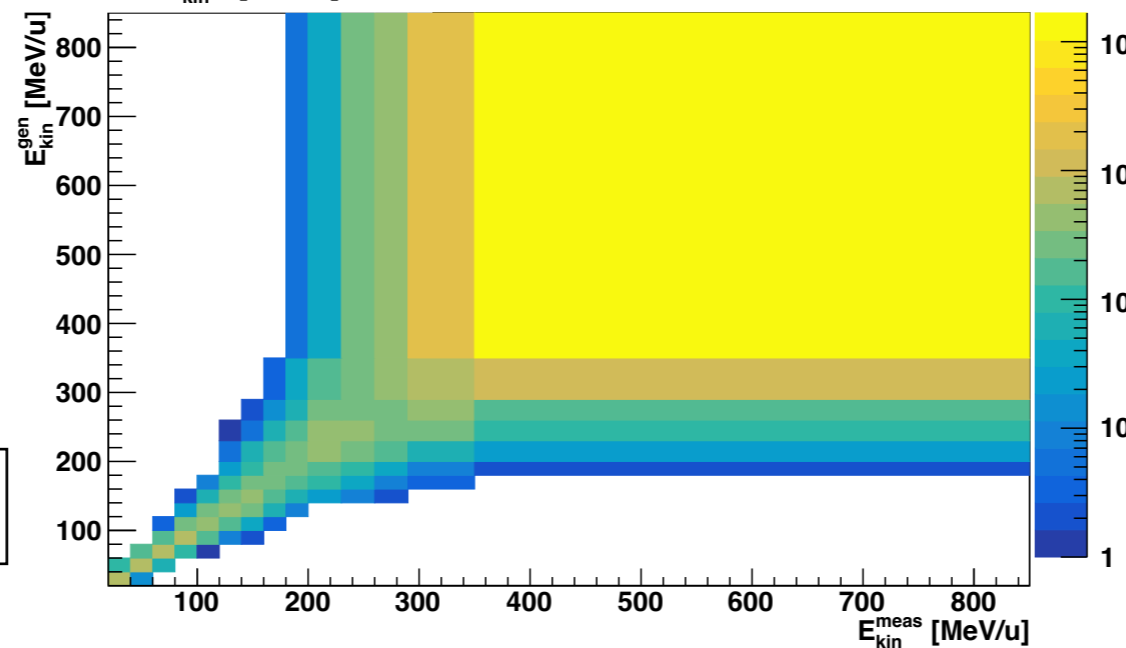
p - C - 60°



d - C - 60°



t - C - 60°

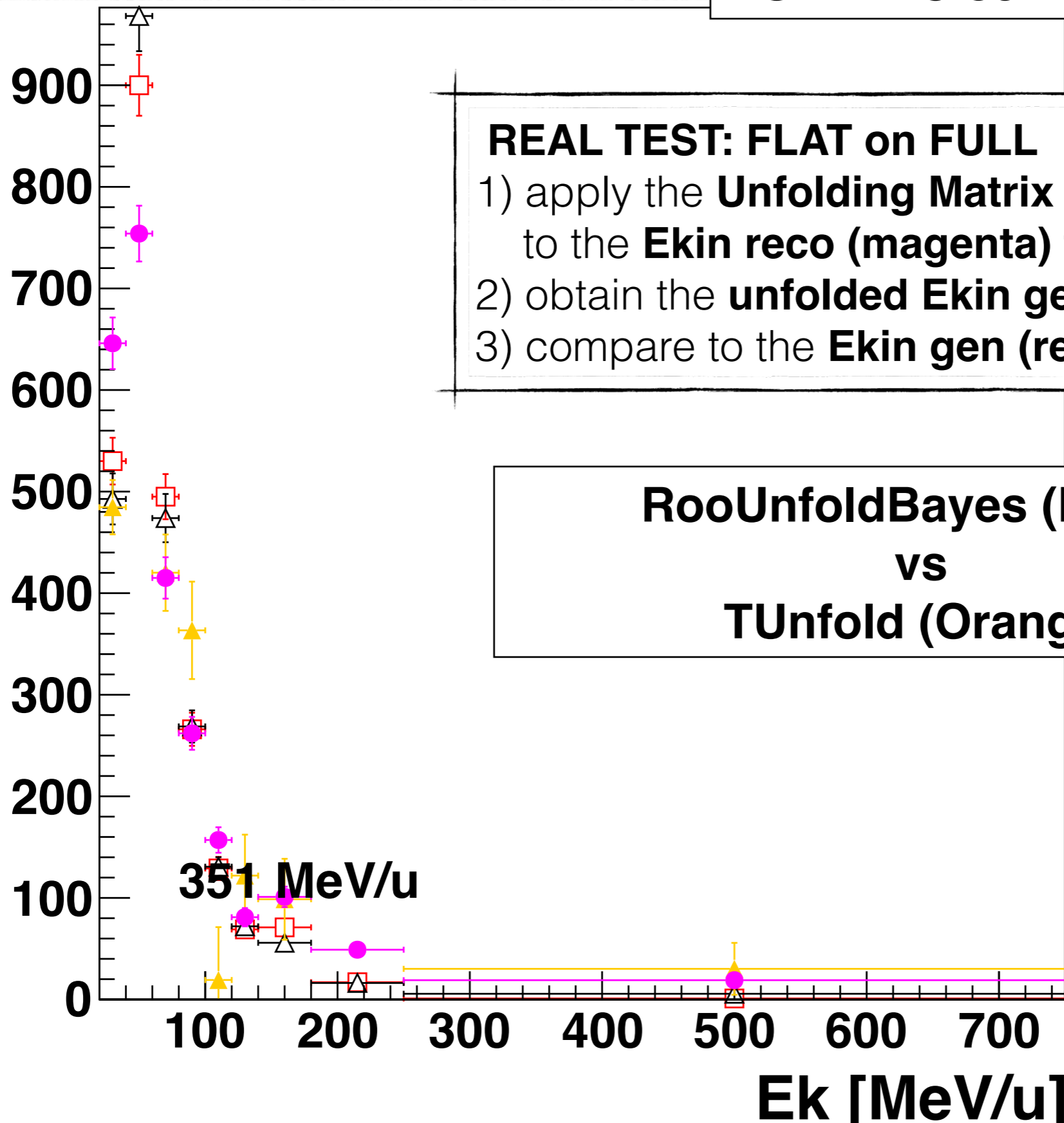


UNFOLDING

FLAT: p - PMMA - 90°

FULL: ^{12}C 351 MeV/u - PMMA - 90°

Entries



REAL TEST: FLAT on FULL

- 1) apply the **Unfolding Matrix** from FLAT MC to the **E_{kin} reco** (magenta) from FULL MC
- 2) obtain the **unfolded E_{kin} gen** (black)
- 3) compare to the **E_{kin} gen** (red) of FULL MC

RooUnfoldBayes (Black)

vs

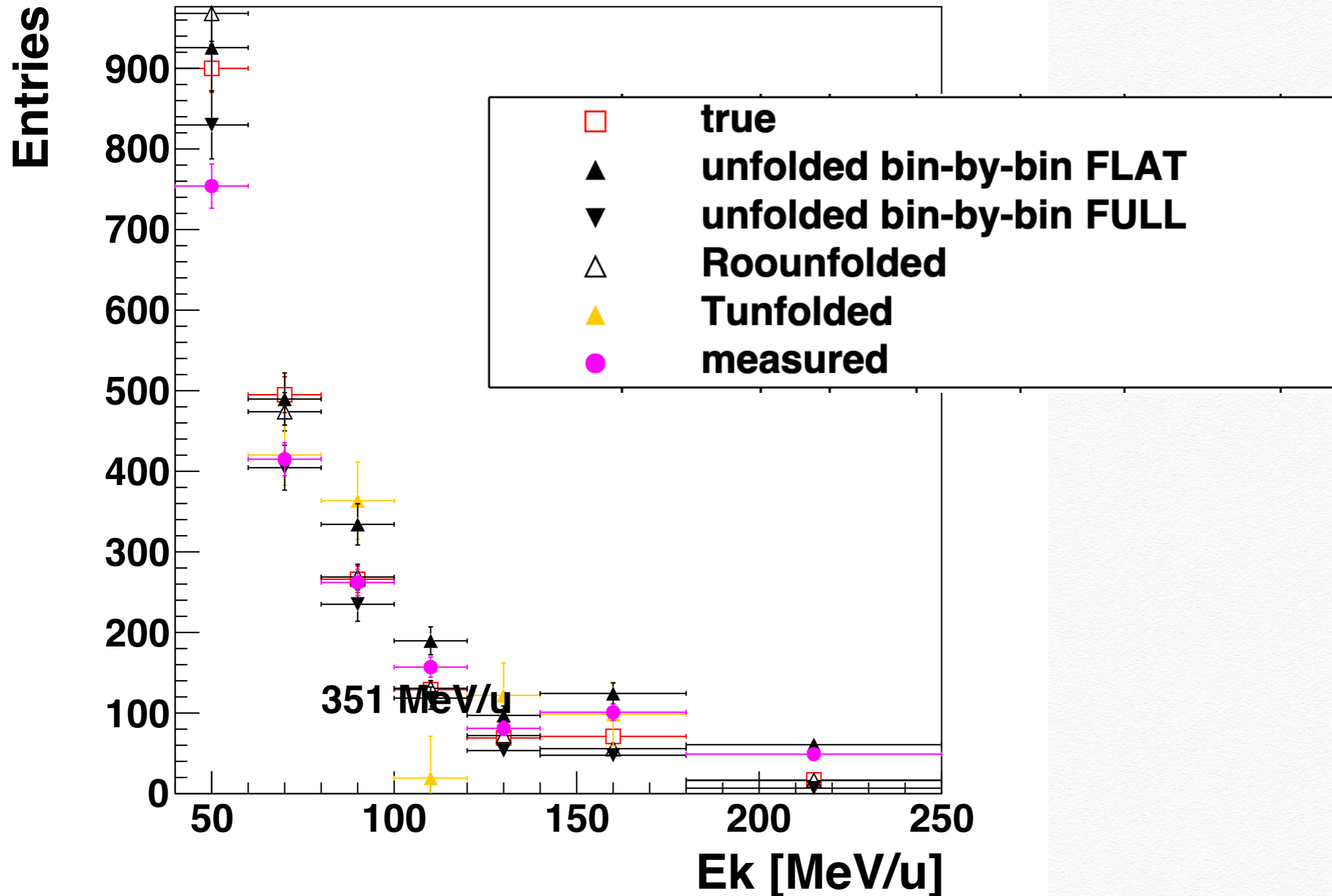
TUnfold (Orange)

351 MeV/u

UNFOLDING

FLAT: p - PMMA - 90°

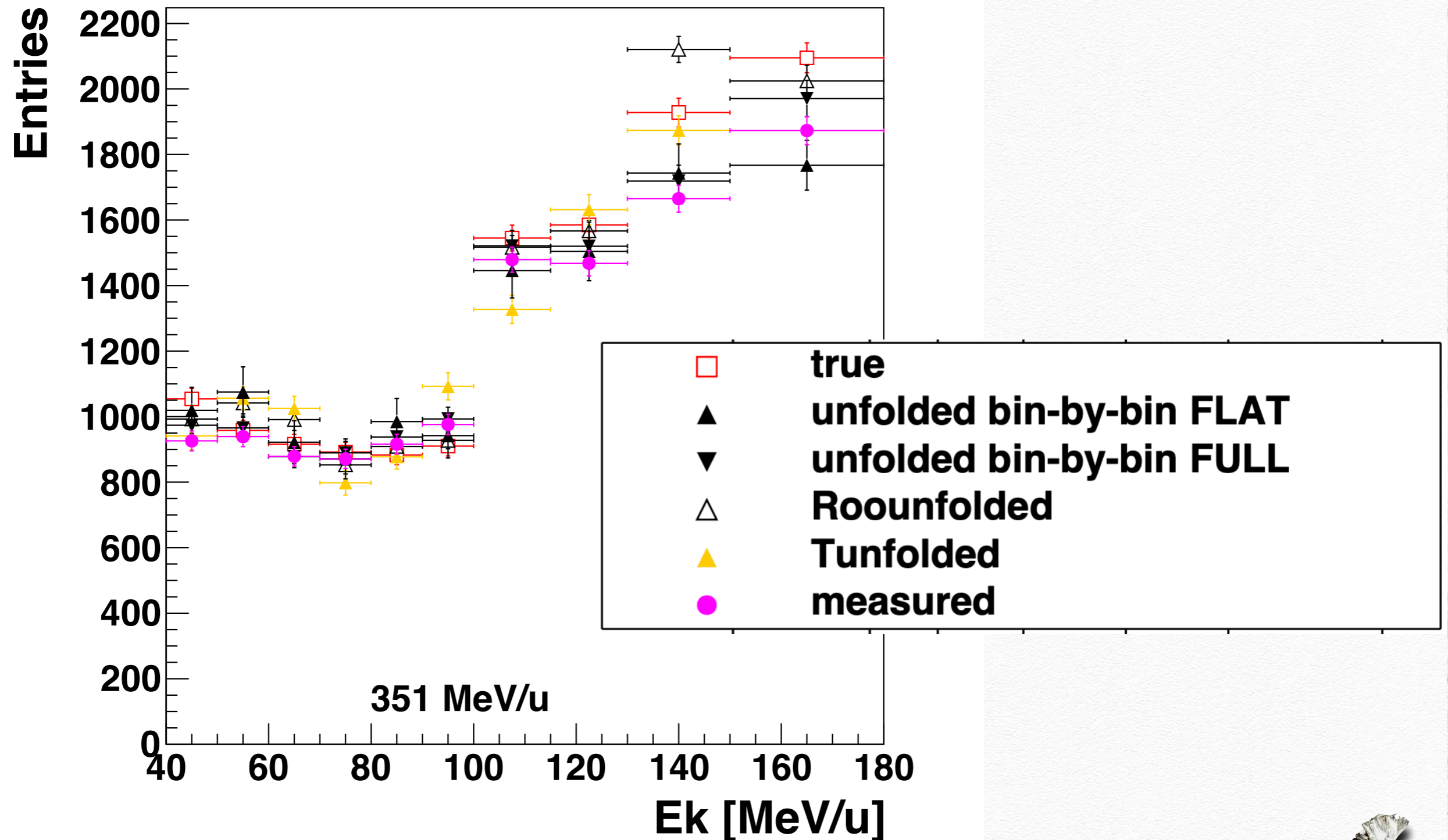
- REAL TEST: FLAT on FULL



UNFOLDING

FLAT: p - C - 32°

- REAL TEST: FLAT on FULL



Cross section 2024 - PURITY

The ^{12}C fragmentation cross sections for a ${}^A_Z X$ fragment are obtained as:

$$\frac{d\sigma}{dE_k} \left(\frac{A}{Z} X \right) = \frac{N_{\frac{A}{Z} X} (E_k)}{\Delta E_k} \cdot \frac{\text{Purity}}{N_{12\text{C}} N_Y} \cdot \frac{1}{\epsilon}$$

$$\text{Purity} = \frac{\text{number of particles selected in } p(d,t) \text{ band}}{\text{number of true } p(d,t) \text{ in } p(d,t) \text{ band}}$$

Purity values range [96 - 100] %

Normalization

The ^{12}C fragmentation cross sections for a ${}^A_Z X$ fragment are obtained as:

$$\frac{d\sigma}{dE_k} \left(\frac{A}{Z} X \right) = \frac{N_{\frac{A}{Z} X} (E_k)}{\Delta E_k} \cdot \overbrace{N_{12C} N_Y}^{\text{Purity}} \cdot \frac{1}{\epsilon}$$

From CNAO
Dose Delivery

Information of the target composition:

Target	Composition	Thickness [mm]	Density [g/cm ³]
PMMA	C ₅ O ₂ H ₈	2	1.19
Graphite	C	1	0.94
Plas.Scint.	C _b H _a	2	1.024

dose-current conversion systematic uncertainty. The relative uncertainty on N_{12C} (4%) is hence the convolution of the uncertainty on the stopping power determination [20] and on the dose measurements [21]. A possible additional contribution to the systematic uncertainty, coming from the monitoring system measurement stability [22], was found to be negligible

$$N_Y = \frac{\rho_Y \cdot th_Y \cdot N_A}{A_Y}$$

$$th_y = th_y^* \sqrt{2}$$

N_{12C}	$\cdot 10^6$	$\cdot 10^6$	$\cdot 10^6$	$\cdot 10^6$	$\cdot 10^6$
Target	115	153	222	281	353
	[MeV/u]	[MeV/u]	[MeV/u]	[MeV/u]	[MeV/u]
PMMA	49866	46512	49395	49601	42000
Graphyte	49454	46583	47484	47288	49328
Plast. Scint.	49728	50600	49347	49787	49653

Efficiency evaluation:

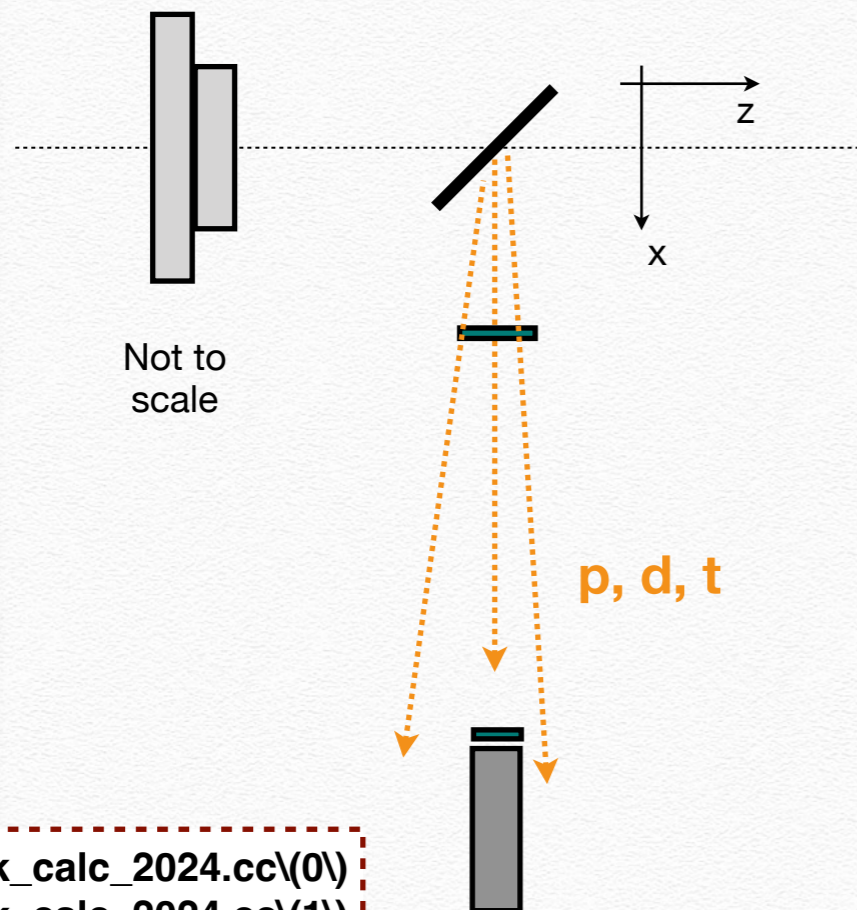
$$\epsilon = \epsilon_{Det} \cdot \epsilon_{Sel} \cdot \epsilon_{DT}$$

The efficiency $\epsilon_{Det}(E_{kin})$ and $\epsilon_{Sel}(E_{kin})$ have been evaluated using dedicated Monte Carlo simulations developed with the FLUKA code

=> MC FULL triggered: at least 1 fragment (idpa = 1 or -3 or -4) born in tgt

◆ To evaluate $\epsilon_{Det}(E_{kin})$: trigger and detector efficiency + geometry

$$\epsilon_{Det}(E_{kin}) = \frac{\epsilon_{Det}^{NUME}}{\epsilon_{Det}^{DENO}}$$



Eps_det_NUME

- Triggered (time coinc btw STSa and STSb < 150 ns && Edep in STSa,b > 100keV)
- Cross STSa, STSb, LYSO
- above detectors (STSa, STSb, LYSO) energy thresholds cuts as data
(90/60°: Ely_cut = 24 MeV, Estsa,b_cut = 5 MeV)
(50/32°: Ely_cut = 24 MeV, Estsa,b_cut = 2,3 MeV)
- Eps_det_DENO selections

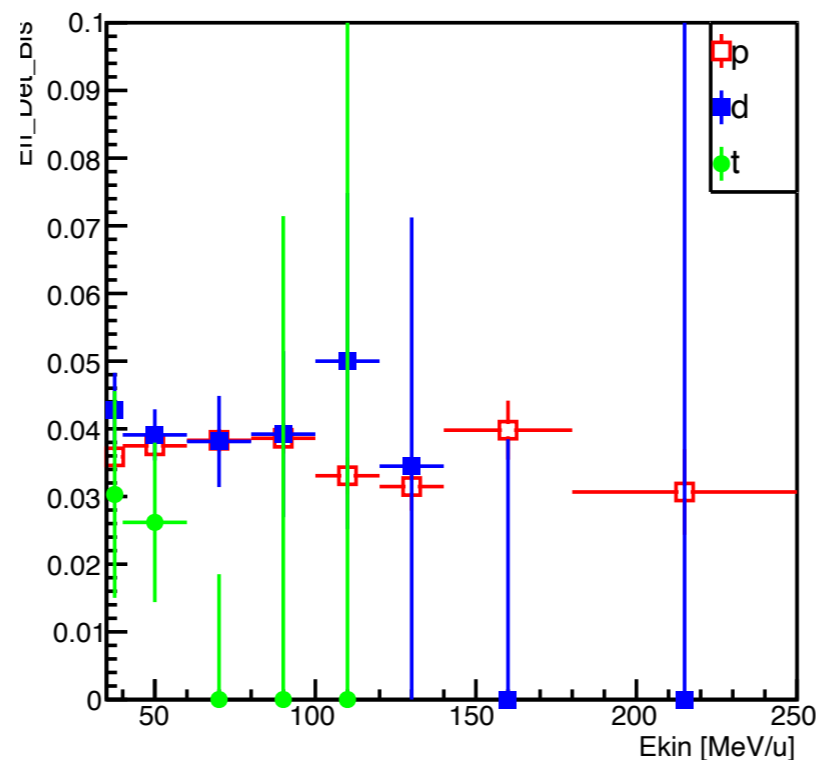
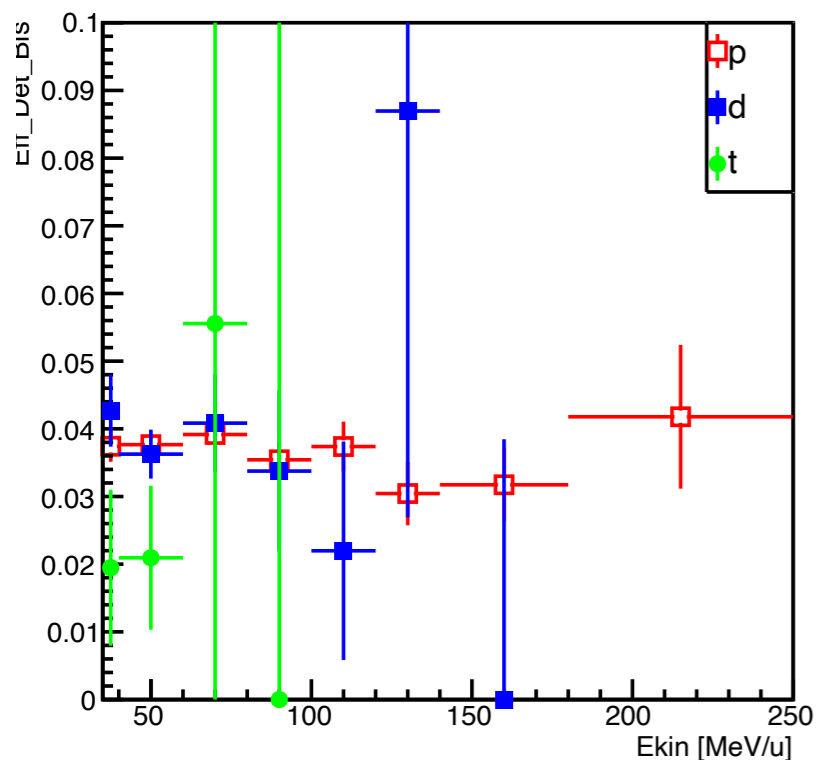
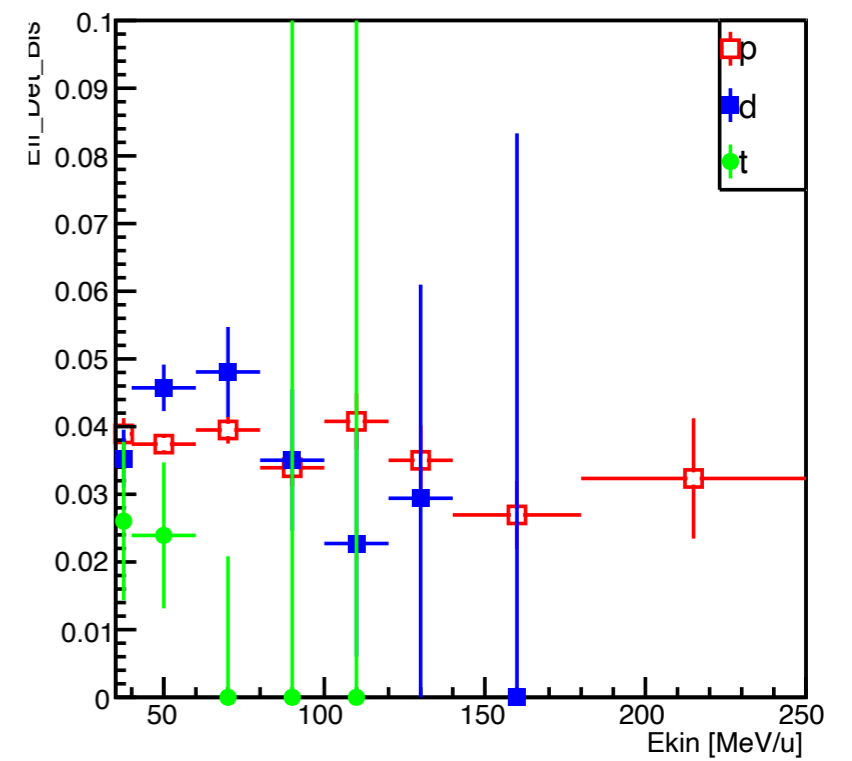
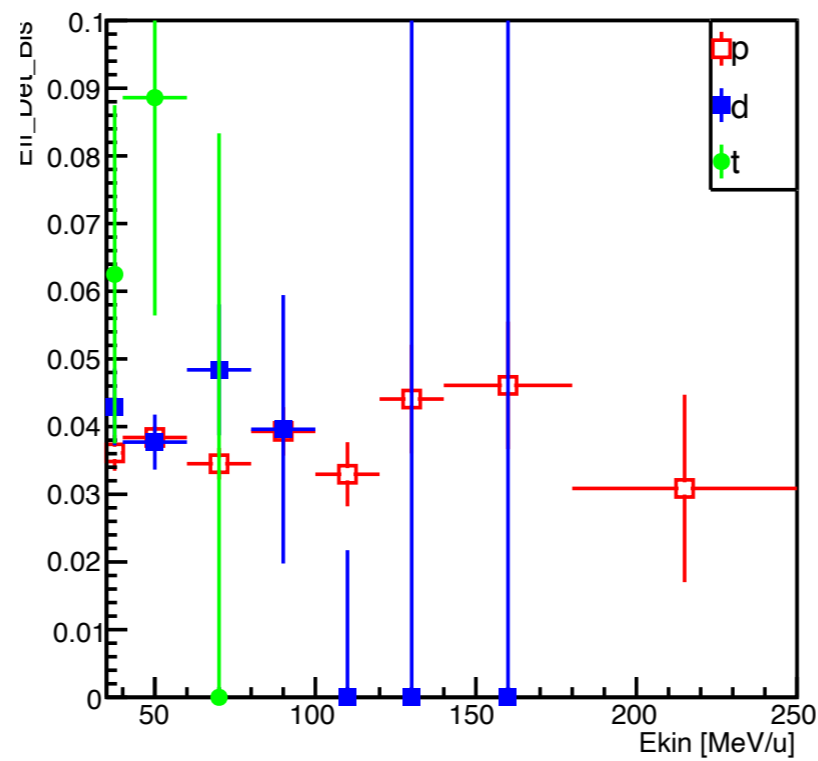
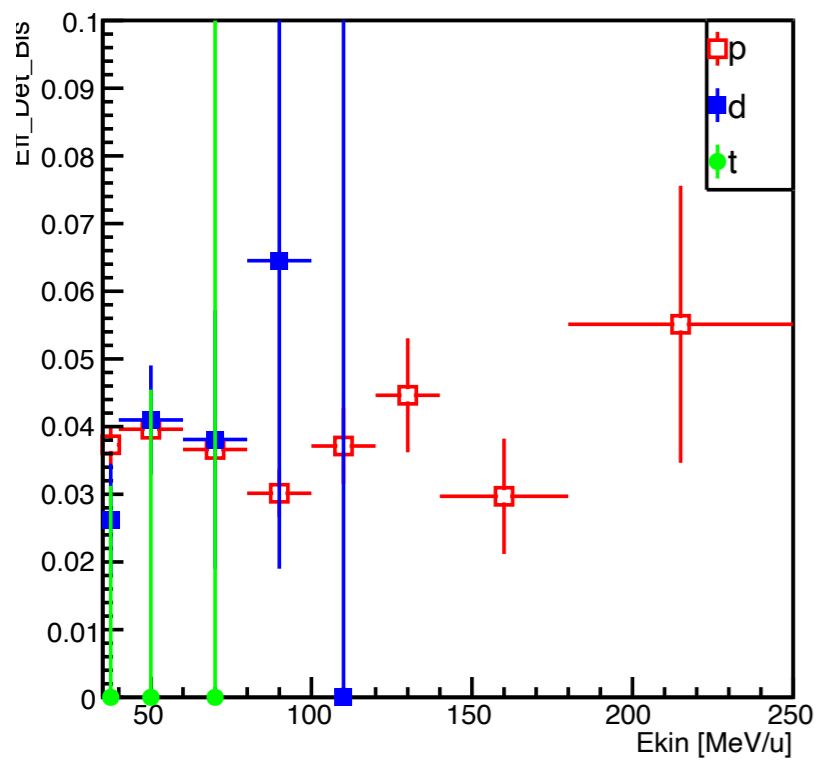
Eps_det_DENO

- p (d, t)
- born in tgt
- son of a primary particle
- out of tgt
- out of tgt in (Theta±DTheta(4°); Phi± DPhi(4°/6°@32deg))

```
root -l effEk_calc_2024.cc\0)
root -l effEk_calc_2024.cc\1)
root -l histos_effdet.cc\0)
root -l histos_effdet.cc\1)
```


Efficiency evaluation:

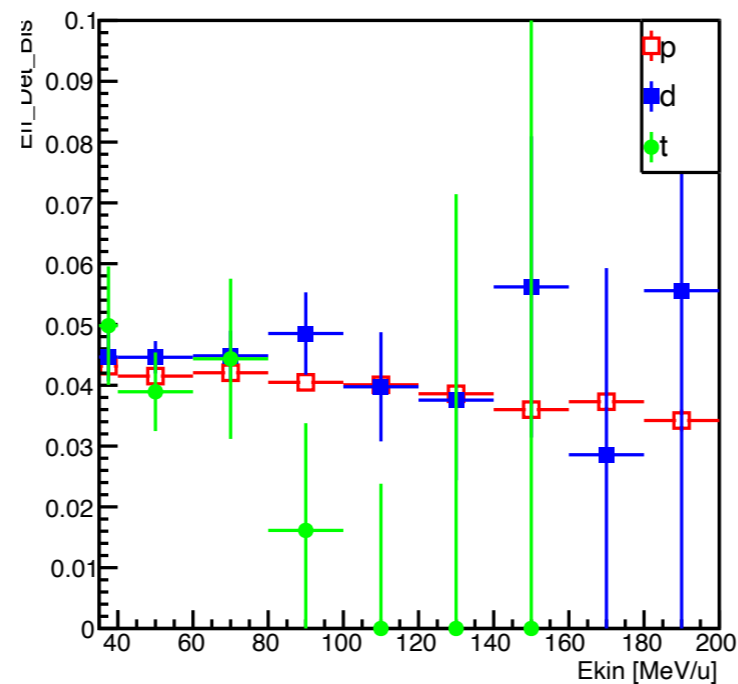
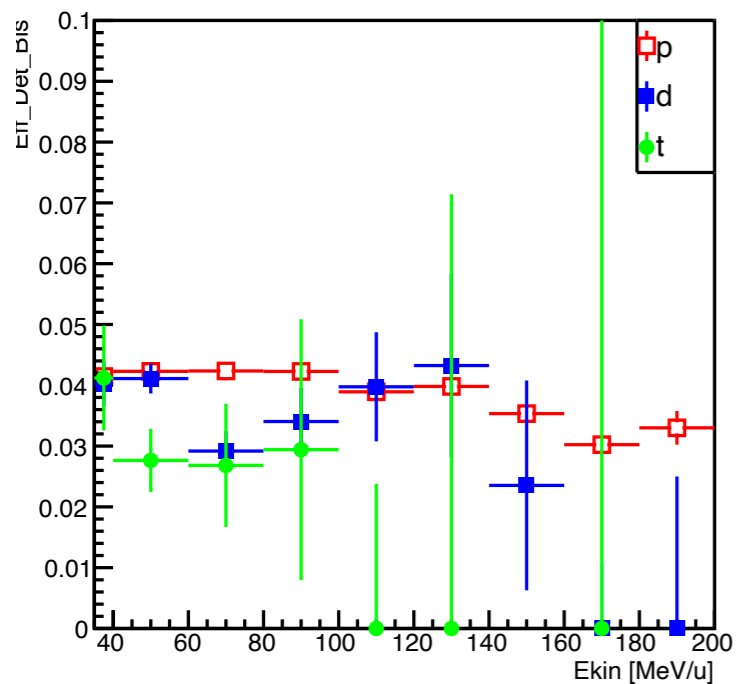
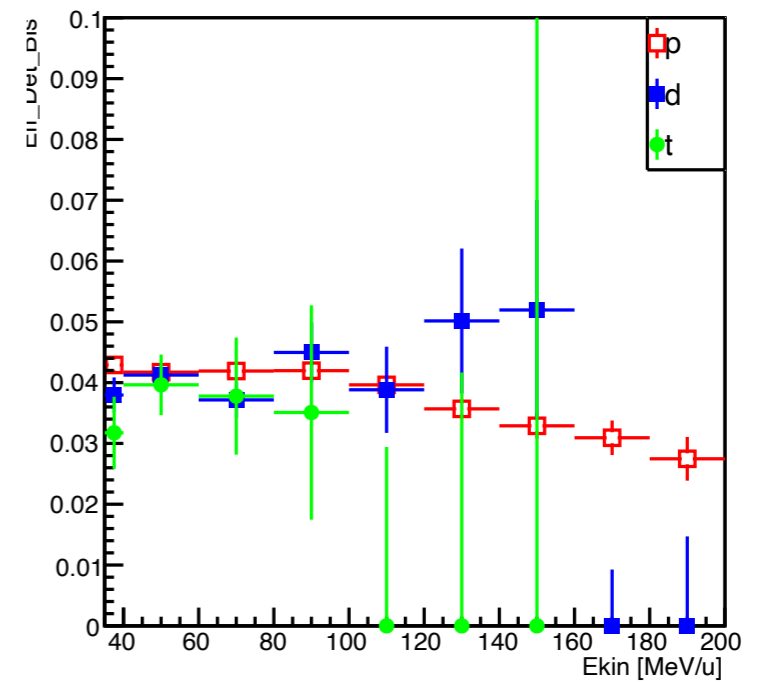
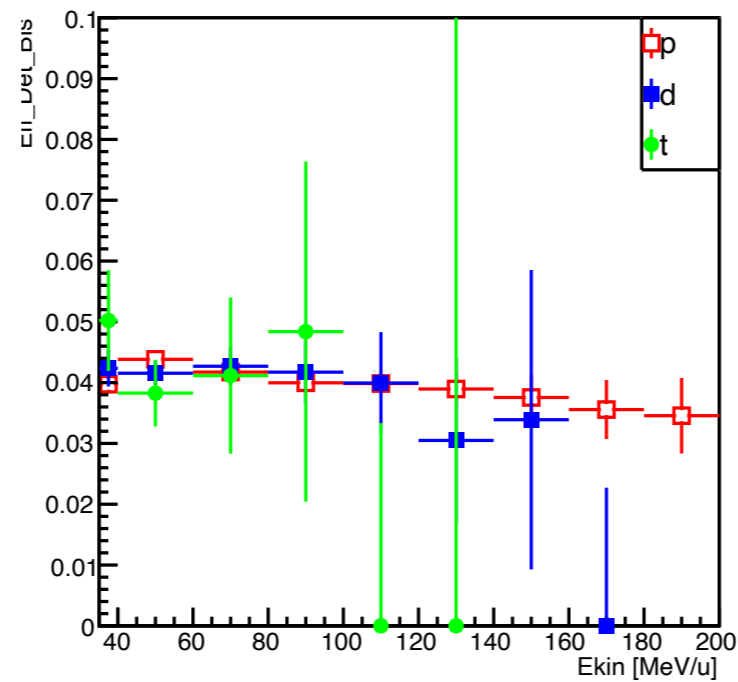
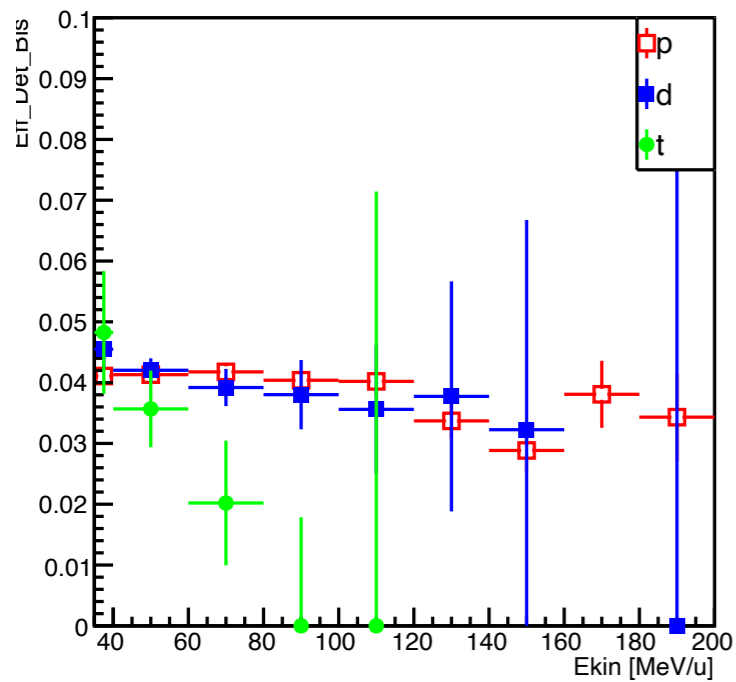
$$\epsilon = \epsilon_{Det} \cdot \epsilon_{Sel} \cdot \epsilon_{DT}$$



90°
PMMA

Efficiency evaluation:

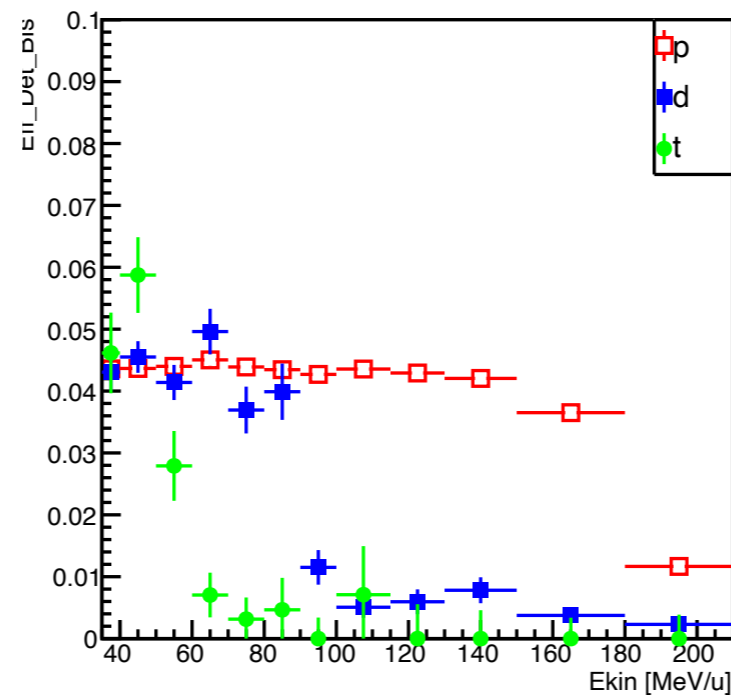
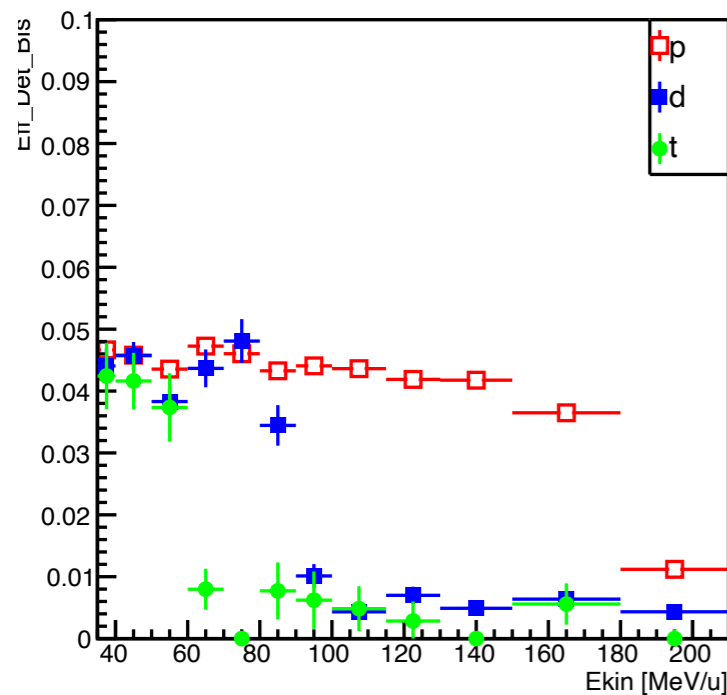
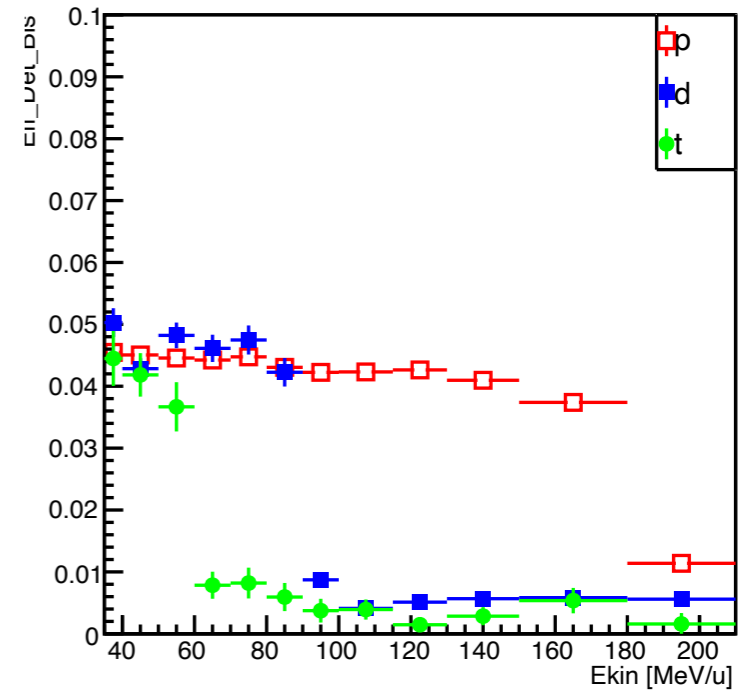
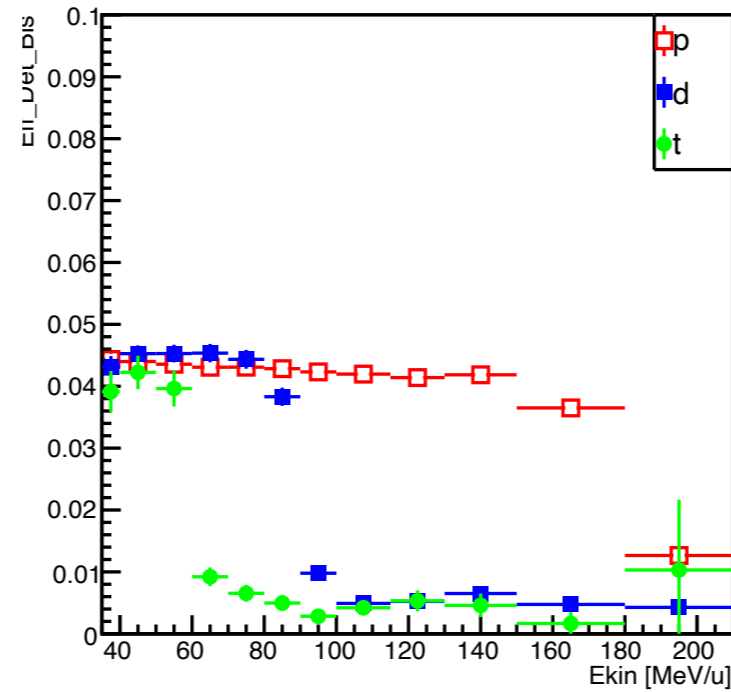
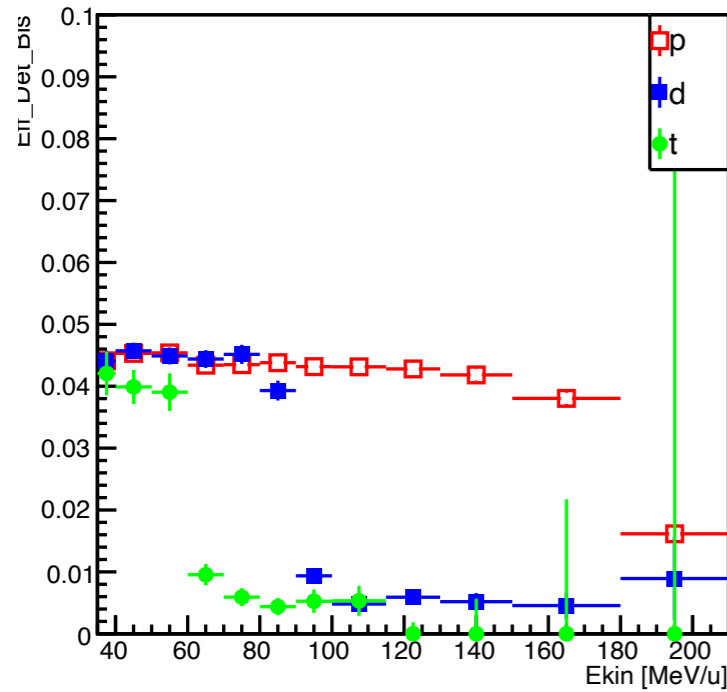
$$\epsilon = \epsilon_{Det} \cdot \epsilon_{Sel} \cdot \epsilon_{DT}$$



60°
PMMA

Efficiency evaluation:

$$\epsilon = \epsilon_{Det} \cdot \epsilon_{Sel} \cdot \epsilon_{DT}$$



32°
PMMA

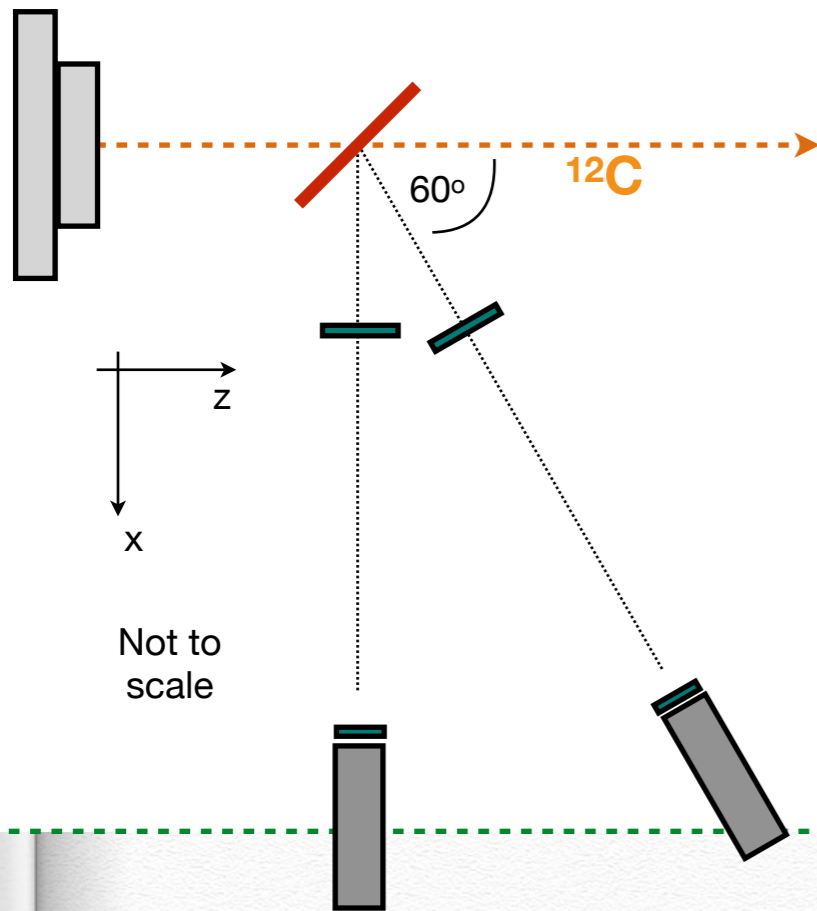
Efficiency evaluation:

$$\epsilon = \epsilon_{Det} \cdot \epsilon_{Sel} \cdot \epsilon_{DT}$$

The efficiency $\epsilon_{Det}(E_{kin})$ and $\epsilon_{Sel}(E_{kin})$ have been evaluated using dedicated Monte Carlo simulations developed with the FLUKA code

=> MC FULL triggered: at least 1 fragment (idpa = 1 or -3 or -4) born in tgt

◆ To evaluate ϵ_{Sel} : p, d, t identification efficiency using the Zid + PID bands



root -l effMix_Ekin_2024_E.cc

Probability that a fragment of type u is measured in the region v ($u, v = p, d, t$)

$$\epsilon_{mix}^{uv} = \frac{N^{uv}}{N^u}$$

Eps_sel_NUME

- in p (d, t) selection, z1 selection, z2 selection
- ● Eps_sel_DENO selections

Eps_sel_DENO = Eps_det_NUME

- Triggered (time coinc btw STSa and STSb < 150 ns && Edep in STSa,b > 100keV)
- Cross STSa, STSb, LYSO
- above detectors (STSa, STSb, LYSO) energy thresholds cuts as data
 - (90/60°: Ely_cut = 24 MeV, Estsa,b_cut = 5 MeV)
 - (50/32°: Ely_cut = 24 MeV, Estsa,b_cut = 2,3 MeV)
- p (d, t)
- born in tgt
- son of a primary particle
- out of tgt
- out of tgt in LYSO acceptance (in cartesian coordinates)

Efficiency evaluation:

$$\epsilon = \epsilon_{Det} \cdot \epsilon_{Sel} \cdot \epsilon_{DT}$$

PMMA 115			
90° — Ekin [MeV]	ϵ_{pp} [%]	ϵ_{dd} [%]	ϵ_{tt} [%]
37.5 ± 2.5	99.4 ± 0.7	80.0 ± 12.4	-
50.0 ± 10.0	99.0 ± 0.5	92.0 ± 5.6	-
70.0 ± 10.0	97.0 ± 1.4	100.0 ± 10.0	-
90.0 ± 10.0	97.2 ± 2.1	50.0 ± 28.9	-
110.0 ± 10.0	95.3 ± 3.3	-	-
130.0 ± 10.0	96.3 ± 3.9	-	-
160.0 ± 20.0	83.3 ± 10.6	-	-
215.0 ± 35.0	71.4 ± 16.2	-	-
60° — Ekin [MeV]	ϵ_{pp} [%]	ϵ_{dd} [%]	ϵ_{tt} [%]
37.5 ± 2.5	99.6 ± 0.2	99.4 ± 0.6	81.8 ± 8.2
50.0 ± 10.0	98.6 ± 0.2	96.4 ± 0.9	96.8 ± 3.4
70.0 ± 10.0	96.7 ± 0.5	89.2 ± 2.5	75.0 ± 20.0
90.0 ± 10.0	95.3 ± 0.8	60.5 ± 7.4	-
110.0 ± 10.0	93.5 ± 1.4	27.3 ± 13.0	-
130.0 ± 10.0	90.8 ± 2.5	25.0 ± 20.0	-
150.0 ± 10.0	86.2 ± 4.5	0.0 ± 25.0	-
170.0 ± 10.0	76.1 ± 6.2	0.0 ± 25.0	-
190.0 ± 10.0	54.5 ± 10.4	-	-
215.0 ± 15.0	61.1 ± 11.2	-	-
245.0 ± 15.0	100.0 ± 16.7	-	-
32° — Ekin [MeV]	ϵ_{pp} [%]	ϵ_{dd} [%]	ϵ_{tt} [%]
37.5 ± 2.5	97.9 ± 0.3	96.2 ± 0.8	87.4 ± 2.9
45.0 ± 5.0	98.2 ± 0.2	94.1 ± 0.7	85.7 ± 2.5
55.0 ± 5.0	98.1 ± 0.2	94.8 ± 0.7	88.0 ± 2.6
65.0 ± 5.0	96.8 ± 0.3	93.7 ± 0.8	51.6 ± 8.8
75.0 ± 5.0	96.0 ± 0.4	92.4 ± 0.9	0.0 ± 2.8
85.0 ± 5.0	95.8 ± 0.4	88.3 ± 1.3	0.0 ± 4.5
95.0 ± 5.0	95.4 ± 0.4	59.4 ± 4.7	0.0 ± 5.6
107.5 ± 7.5	94.9 ± 0.4	19.2 ± 5.4	0.0 ± 8.3
122.5 ± 7.5	93.0 ± 0.6	3.2 ± 3.4	-
140.0 ± 10.0	90.0 ± 0.7	0.0 ± 3.3	-
165.0 ± 15.0	80.0 ± 1.2	0.0 ± 8.3	-

PMMA 115						
90° — Ekin [MeV]	ϵ_{dp} [%]	ϵ_{tp} [%]	ϵ_{pd} [%]	ϵ_{td} [%]	ϵ_{pt} [%]	ϵ_{dt} [%]
37.5 ± 2.5	0.6 ± 0.7	0.0 ± 0.3	0.0 ± 4.5	0.0 ± 4.5	-	-
50.0 ± 10.0	0.2 ± 0.3	0.0 ± 0.1	0.0 ± 1.9	0.0 ± 1.9	-	-
70.0 ± 10.0	0.0 ± 0.3	0.0 ± 0.3	0.0 ± 10.0	0.0 ± 10.0	-	-
90.0 ± 10.0	0.0 ± 0.7	0.0 ± 0.7	0.0 ± 16.7	0.0 ± 16.7	-	-
110.0 ± 10.0	0.0 ± 1.1	0.0 ± 1.1	-	-	-	-
130.0 ± 10.0	0.0 ± 1.8	0.0 ± 1.8	-	-	-	-
160.0 ± 20.0	0.0 ± 3.8	0.0 ± 3.8	-	-	-	-
215.0 ± 35.0	0.0 ± 6.2	0.0 ± 6.2	-	-	-	-
60° — Ekin [MeV]	ϵ_{dp} [%]	ϵ_{tp} [%]	ϵ_{pd} [%]	ϵ_{td} [%]	ϵ_{pt} [%]	ϵ_{dt} [%]
37.5 ± 2.5	0.0 ± 0.1	0.1 ± 0.1	0.0 ± 0.3	1.1 ± 0.8	0.0 ± 2.2	4.5 ± 4.8
50.0 ± 10.0	0.3 ± 0.1	0.0 ± 0.0	0.0 ± 0.1	0.2 ± 0.3	0.0 ± 1.6	9.7 ± 5.4
70.0 ± 10.0	0.3 ± 0.1	0.0 ± 0.0	0.0 ± 0.3	0.0 ± 0.3	0.0 ± 10.0	225.0 ± 10.0
90.0 ± 10.0	0.3 ± 0.2	0.0 ± 0.1	0.0 ± 1.1	0.0 ± 1.1	-	-
110.0 ± 10.0	0.0 ± 0.2	0.0 ± 0.2	0.0 ± 4.2	0.0 ± 4.2	-	-
130.0 ± 10.0	0.0 ± 0.4	0.0 ± 0.4	0.0 ± 10.0	0.0 ± 10.0	-	-
150.0 ± 10.0	0.0 ± 0.8	0.0 ± 0.8	0.0 ± 25.0	0.0 ± 25.0	-	-
170.0 ± 10.0	0.0 ± 1.1	0.0 ± 1.1	300.0 ± 25.0	0.0 ± 25.0	-	-
190.0 ± 10.0	0.0 ± 2.2	0.0 ± 2.2	-	-	-	-
215.0 ± 15.0	0.0 ± 2.6	0.0 ± 2.6	-	-	-	-
245.0 ± 15.0	0.0 ± 16.7	0.0 ± 16.7	-	-	-	-
32° — Ekin [MeV]	ϵ_{dp} [%]	ϵ_{tp} [%]	ϵ_{pd} [%]	ϵ_{td} [%]	ϵ_{pt} [%]	ϵ_{dt} [%]
37.5 ± 2.5	0.5 ± 0.2	0.2 ± 0.1	0.2 ± 0.2	1.6 ± 0.5	0.0 ± 0.4	0.0 ± 0.4
45.0 ± 5.0	0.7 ± 0.1	0.1 ± 0.1	0.0 ± 0.0	1.2 ± 0.3	0.0 ± 0.2	0.0 ± 0.2
55.0 ± 5.0	0.8 ± 0.2	0.3 ± 0.1	0.0 ± 0.0	0.6 ± 0.2	0.0 ± 0.3	0.0 ± 0.3
65.0 ± 5.0	1.0 ± 0.2	0.3 ± 0.1	0.2 ± 0.2	0.5 ± 0.2	3.2 ± 3.4	9.7 ± 5.4
75.0 ± 5.0	0.9 ± 0.2	0.2 ± 0.1	0.1 ± 0.1	1.1 ± 0.4	0.0 ± 2.8	29.4 ± 10.8
85.0 ± 5.0	0.9 ± 0.2	0.0 ± 0.0	0.0 ± 0.1	1.4 ± 0.5	0.0 ± 4.5	100.0 ± 4.5
95.0 ± 5.0	1.2 ± 0.2	0.1 ± 0.1	1.9 ± 1.4	3.8 ± 1.9	0.0 ± 5.6	12.5 ± 11.8
107.5 ± 7.5	1.2 ± 0.2	0.0 ± 0.0	0.0 ± 0.9	0.0 ± 0.9	0.0 ± 8.3	0.0 ± 8.3
122.5 ± 7.5	0.8 ± 0.2	0.0 ± 0.0	0.0 ± 1.6	0.0 ± 1.6	-	-
140.0 ± 10.0	0.5 ± 0.2	0.0 ± 0.0	0.0 ± 3.3	0.0 ± 3.3	-	-
165.0 ± 15.0	0.2 ± 0.1	0.0 ± 0.0	100.0 ± 8.3	0.0 ± 8.3	-	-

Closure TEST

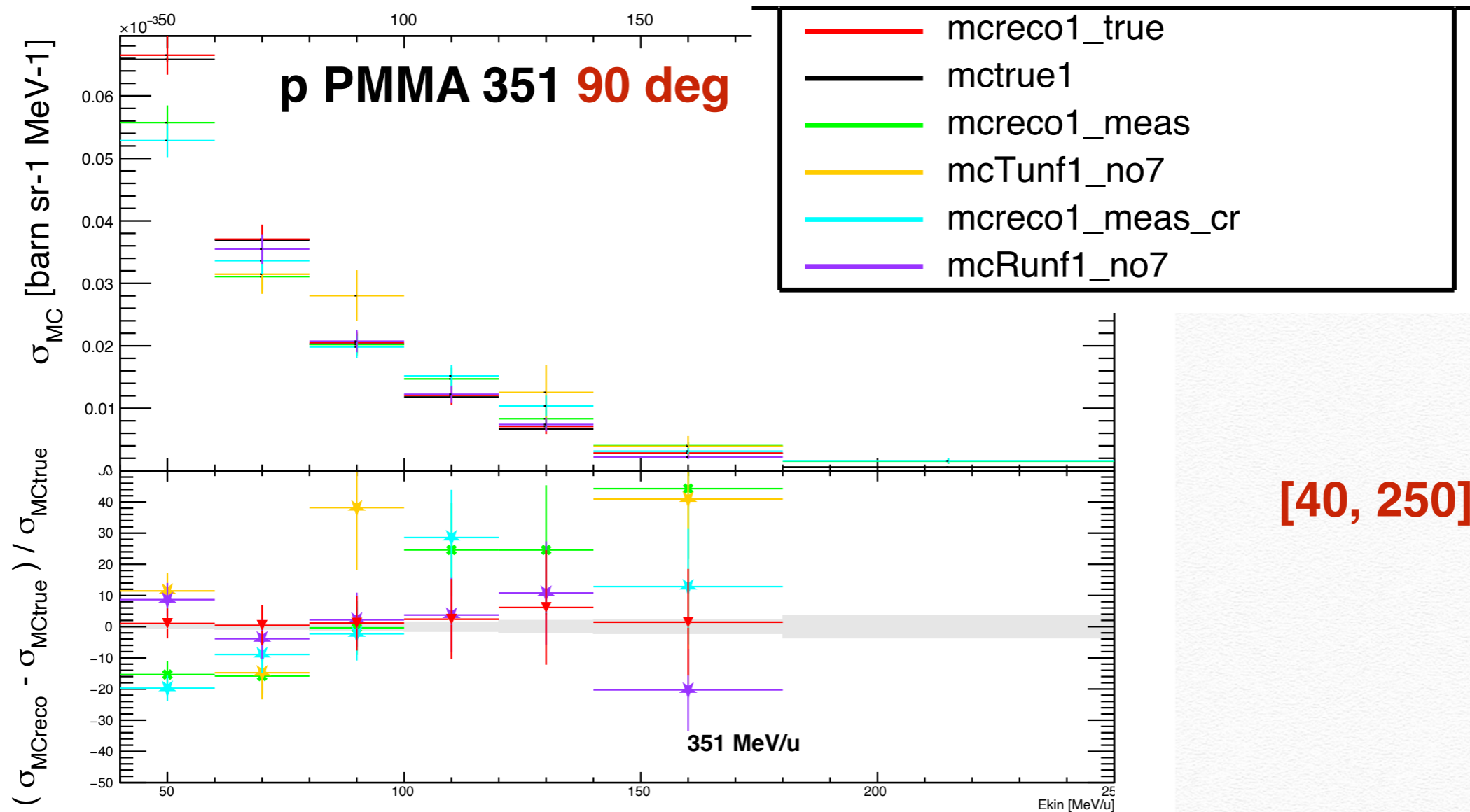
To study the **Monte Carlo reliability** in assessing the efficiencies to be applied to experimental data, we perform the MC Closure Test:

- define the **MC truth** (EpsDet_DENO) = $p(d, t)$,
born in tgt, son of a primary particle,
out of tgt in ($\theta \pm \Delta\theta(4^\circ)$; $\Phi \pm \Delta\Phi(4^\circ/6^\circ@32\text{deg})$)
[no angular bin due to Multiple Scattering]
- **reconstruction of the MC** with efficiencies applied

$$\Rightarrow \text{CLOSURE TEST: } \frac{|\text{MCreco} - \text{MCtruth}|}{\text{MCtruth}}$$

Closure TEST

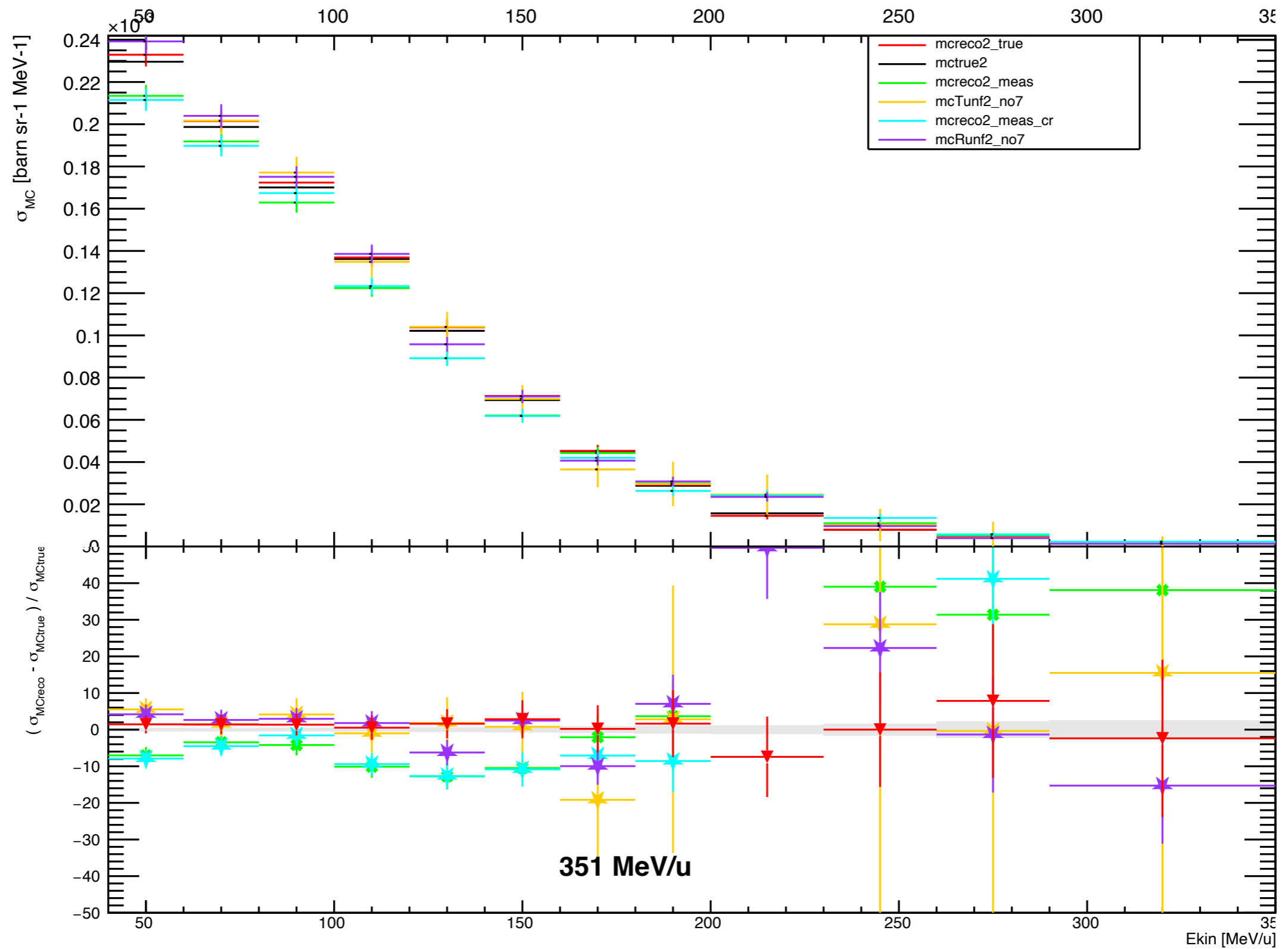
- mctrue = mc @ generation
- mcreco_meas = mc reco (no IDmatch) (Ekin MEAS)
- mcreco_true = mc reco IDmatch (Ekin GEN)
- mcreco_meas_cr = mc reco IDmatch (Ekin MEAS)
- mcTunf = mcreco_meas UNFOLDED with TUnfold (Ekin@gen)
- mcRoounf = mcreco_meas UNFOLDED with RooUnfold (Ekin@gen)



[40, 250] MeV/u

Closure MC

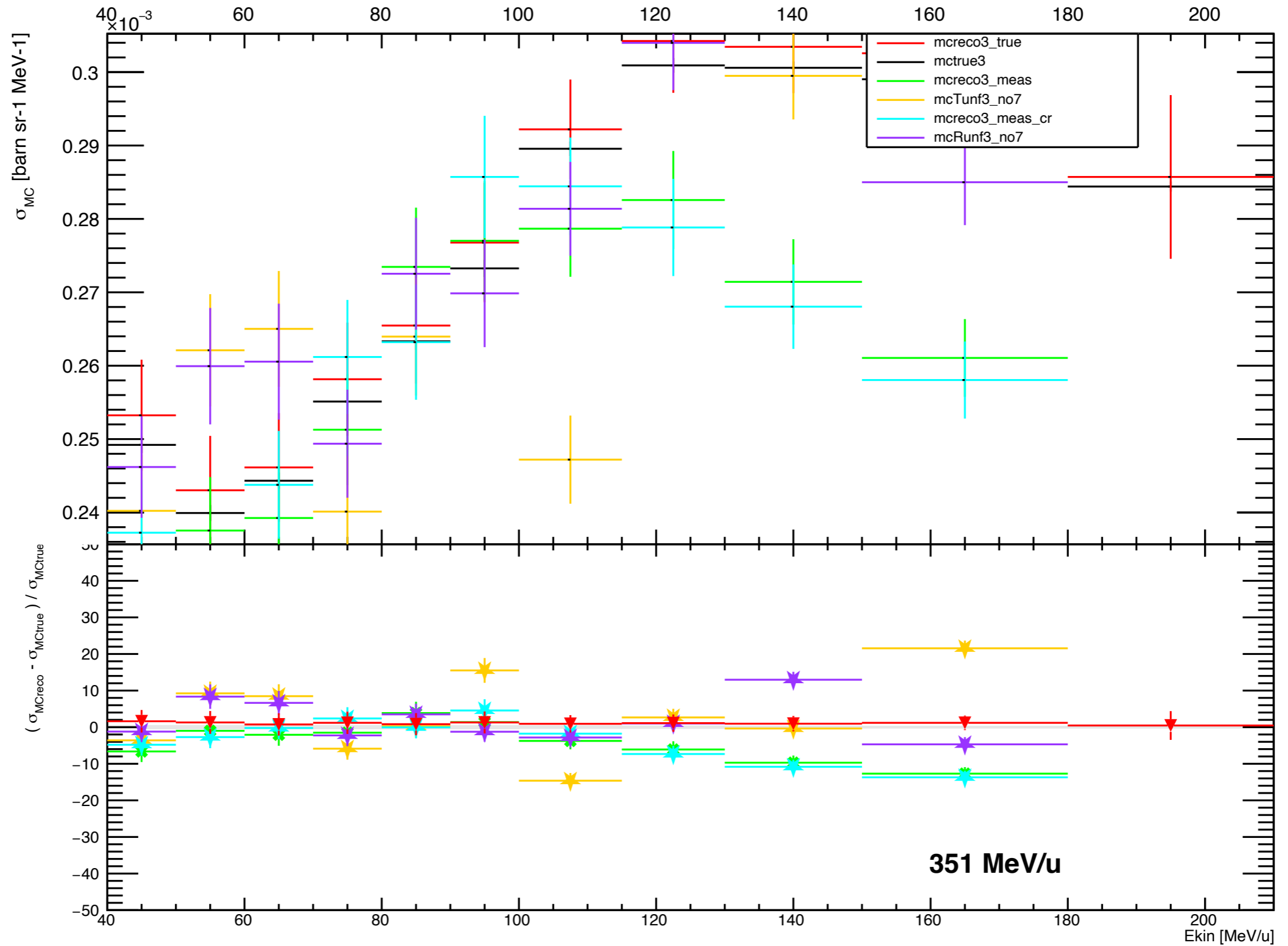
p PMMA 351 60 deg



[40, 350] MeV/u

Closure MC

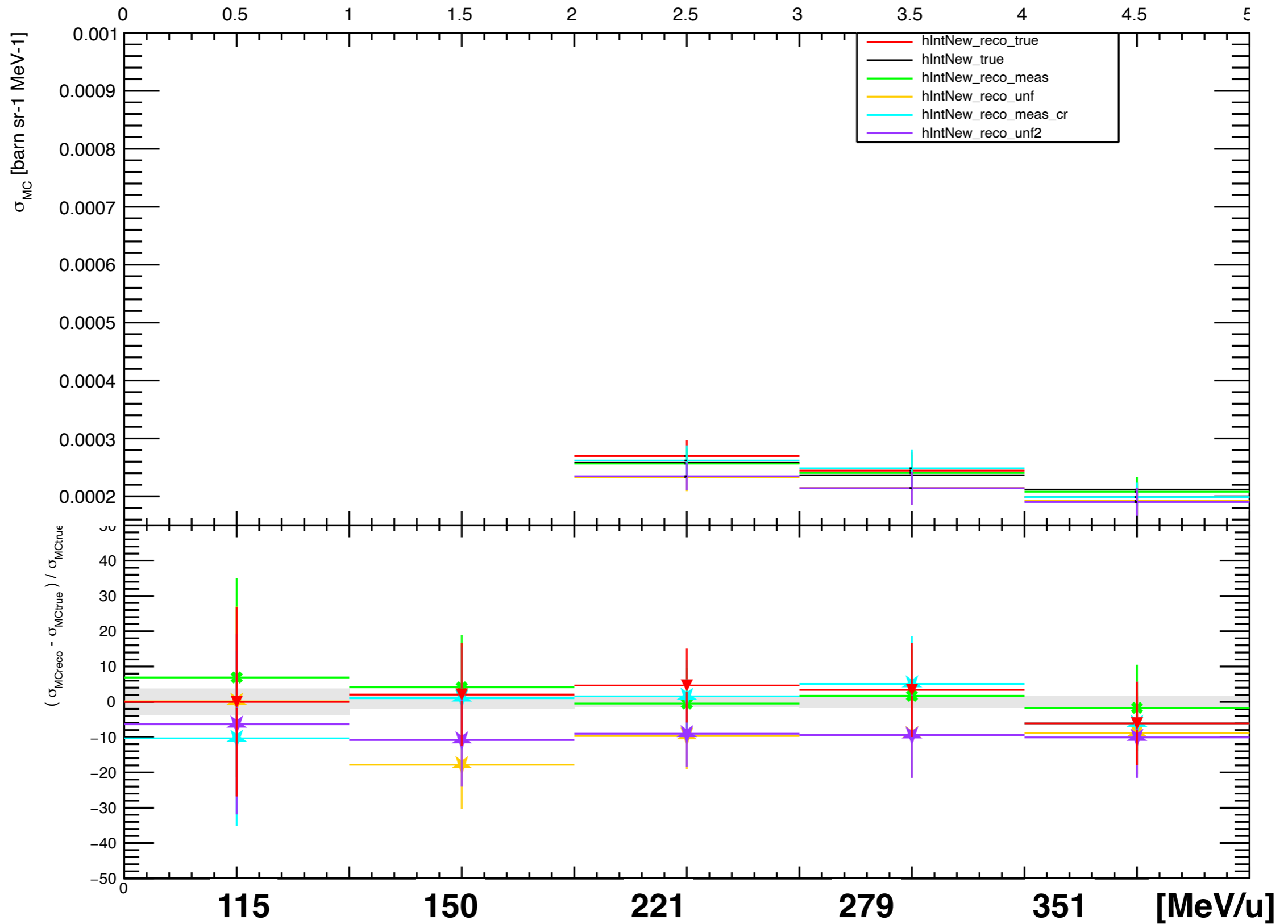
p PMMA 351 32 deg



[40, 180] MeV/u

Closure MC

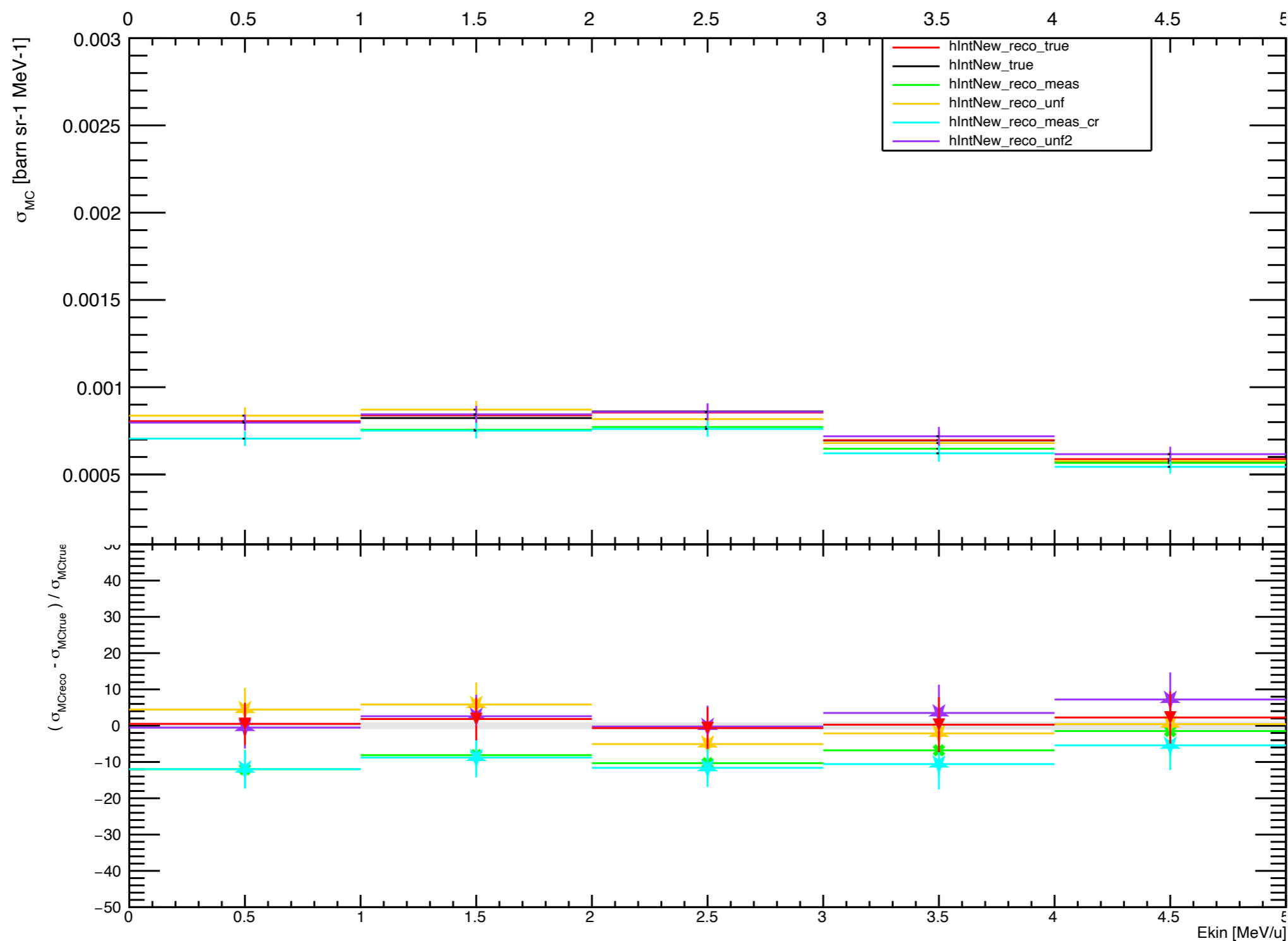
d PMMA Integral 90 deg



[40., 250.] MeV/u

Closure MC

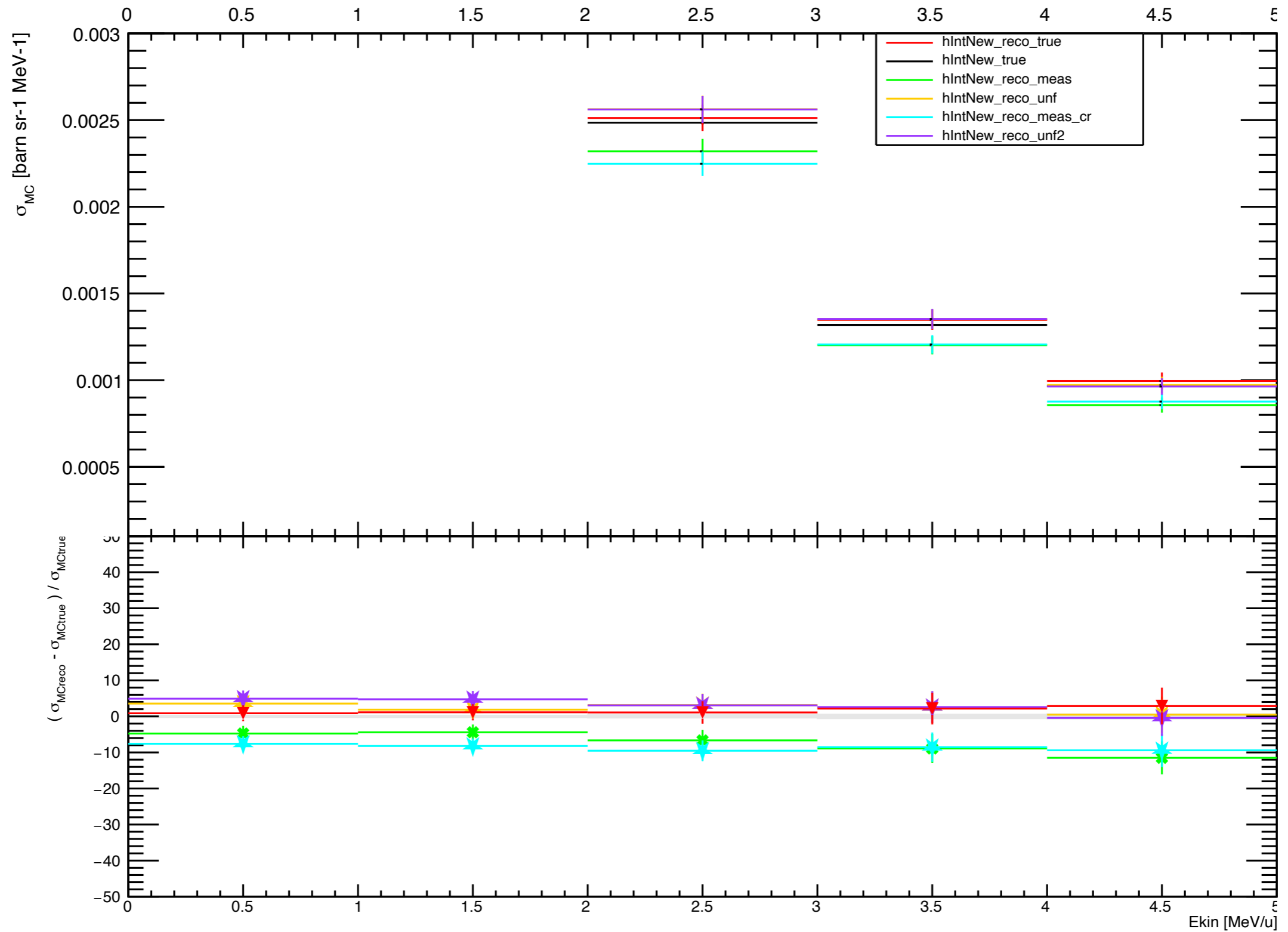
d PMMA Int 60 deg



[40., 350.] MeV/u

Closure MC

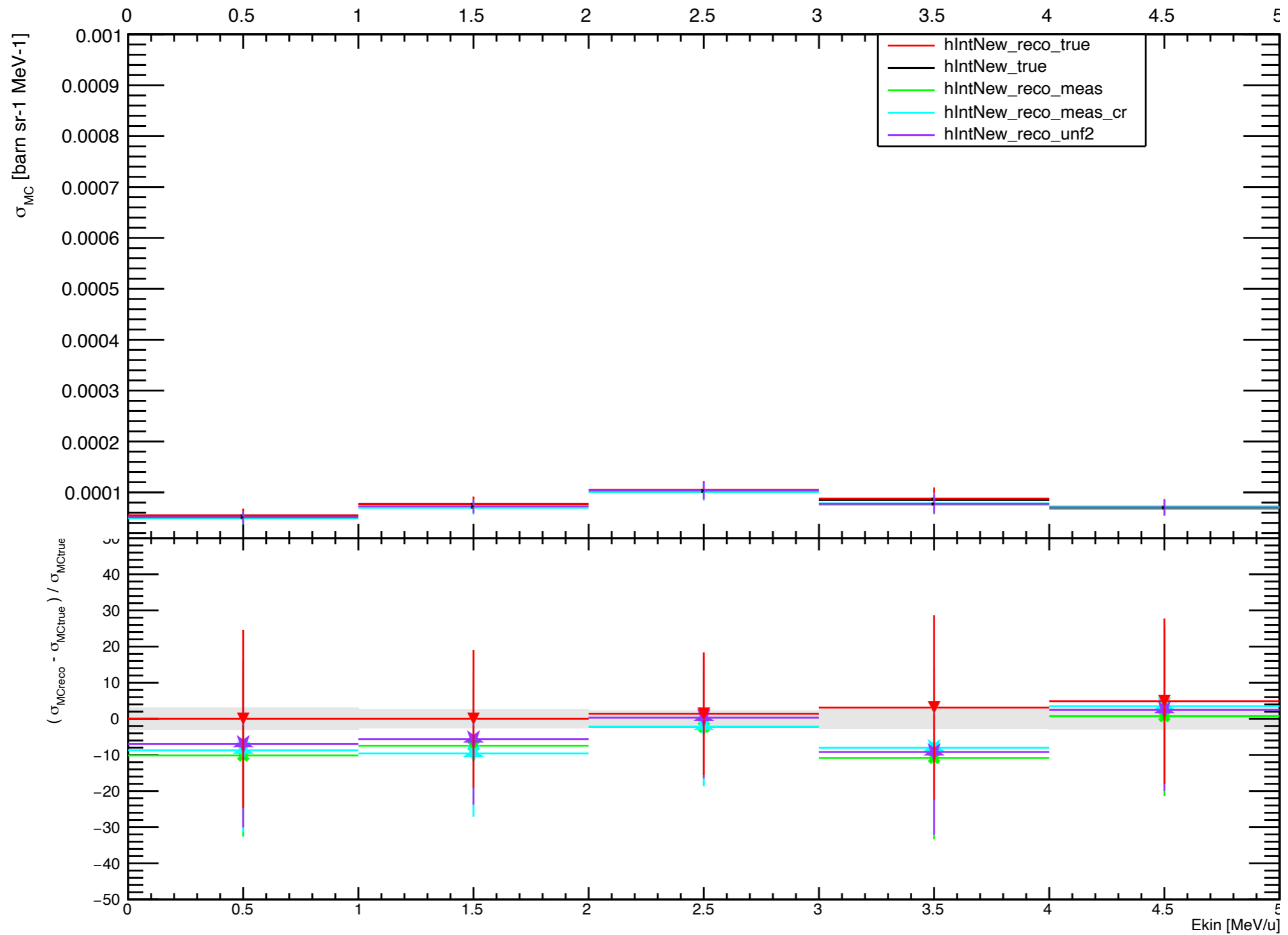
d PMMA Int 32 deg



[40., 90.] MeV/u

Closure MC

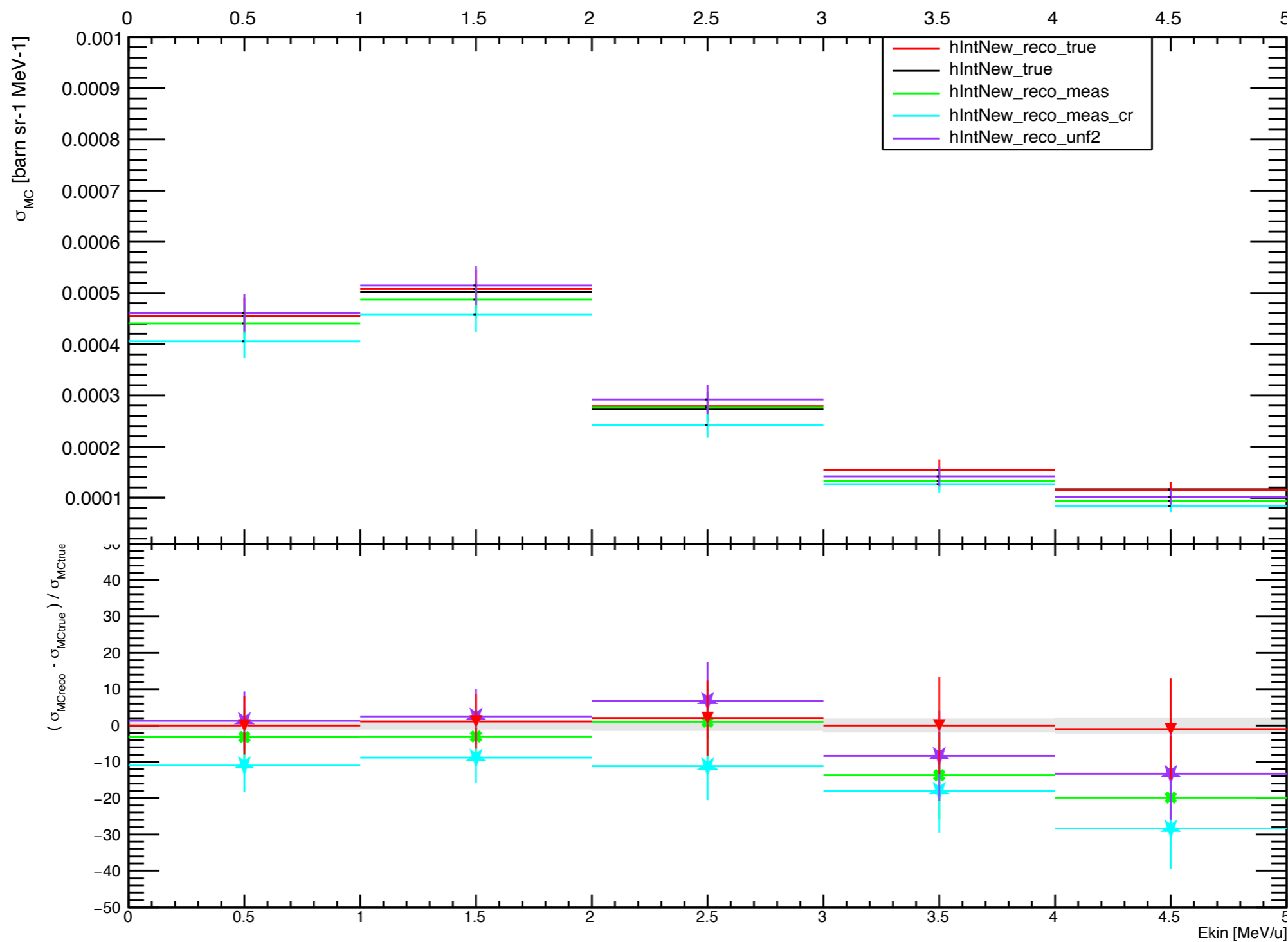
t PMMA Int 60 deg



[40., 350.] MeV/u

Closure MC

t PMMA Int 32 deg



[40., 60.] MeV/u

Conclusions

- **We are performing a study on RooUnfoldBayes to assess the best n iteration parameter which made the unfolding stable also at 32 degrees** (by now we used niter = 3)
- Once the unfolding procedure is stable we will:
 - 1) assess the MCsys error from the closure test
 - 2) apply the unfolding to experimental data
 - 3) add the sys errors to experimental data (machinery ready):
N12C (4%), Closure MC, PID sys, Unfolding sys (?)

